Geomorphology 332 (2019) 138–156

Contents lists available at ScienceDirect

Geomorphology

journal homepage: www.elsevier.com/locate/geomorph

Differentiating the effects of logging, river engineering, and hydropower dams on flooding in the Skokomish River, Washington, USA

Brian D. Collins [a,*], Susan E. Dickerson-Lange [b,1], Sarah Schanz [a,2], Shawn Harrington [a,3]

[a] Department of Earth and Space Sciences, University of Washington, Seattle, WA, United States of America
[b] Department of Civil and Environmental Engineering, University of Washington, Seattle, WA, United States of America

ARTICLE INFO

Article history:
Received 13 September 2018
Received in revised form 31 January 2019
Accepted 31 January 2019
Available online 04 February 2019

Keywords:
Fluvial geomorphology
Downstream effects of hydroelectric dams
Flooding
Channel aggradation
River channel change

ABSTRACT

A decades-long, progressive loss of channel capacity in the Skokomish River, a 622 km^2 basin draining the southeast Olympic Mountains of Washington State, has caused increasing flooding with severe consequences to endangered salmon runs, infrastructure, and private property. To differentiate among multiple potential drivers of the capacity loss, we analyze the geomorphic evidence for the potential effects of: flow regulation by two dams constituting the Cushman Hydroelectric Project, which began regulating flow in the river's North Fork in 1925 and diverting water out of the basin in 1930; sediment production from mid-twentieth century logging in the river's South Fork basin; and twentieth century river engineering in the mainstem. Bankfull channel capacity in the mainstem has steadily declined since about 1940 from 370 m^3 s^{-1} to <100 m^3 s^{-1} due partly to the narrowing of the Skokomish River, which in 2015 was only 45% as wide as it was in 1938. The capacity loss is also due to sediment filling the channel, with nearly 2 m of aggradation measured at a stream gauge since 1965. Comparison of channel cross sections surveyed in 1994, 2007, and 2016 show that about 20,000 m^3 yr^{-1} (34,000 Mg yr^{-1}) of sediment is accumulating in the Skokomish River. The nature, timing, and spatial pattern of this channel narrowing and shallowing are consistent with the response expected from the Cushman Project, which exports water out of basin and thus substantially reduces downstream flows, but, because the dams were built below a natural lake, does not reduce the sediment supply. While sediment yield from the South Fork is high, accounting for about three-fourths of the total sediment supplied to the Skokomish River, it is dominated by the progressive widening of the channel and recruitment by lateral fluvial erosion of glacial sediments in alluvial terraces; landslides associated with logging in the South Fork basin produced a small amount of sediment relative both to the sediment produced by channel widening in the upper South Fork and to the rate of aggradation in the mainstem Skokomish River. The naturally-high sediment load from the South Fork and the flow reduction in the North Fork result in the unusual effect of flooding having increased downstream of the dams despite substantial reductions to peak flows. This case study illustrates how a watershed-scale analysis of multiple land uses and flow management and their interaction with the basin's geology and geomorphology can make use of geomorphic evidence to differentiate among the possible drivers of channel change and associated flooding.

1. Introduction

The Skokomish River, which drains 622 km^2 of the southeast Olympic Mountains into Hood Canal, an arm of Puget Sound in western Washington (Fig. 1), floods multiple times annually and with increasing frequency; the river has crested above flood stage 126 times in the last 20 yr (WY 1998–2017), 51 times in the last 5 yr (WY 2013–2017) and 28 times in the last 2 yr (NOAA, 2018), or 6.3, 10.2 and 14 times yr^{-1}, respectively. The frequent flooding damages farmland and threatens infrastructure. It also endangers salmon runs in both summer and winter: in summer and early fall of most years, the channel dewaters, blocking salmon access to upstream habitat (Fig. 2A), and during late fall and winter floods, when the bulk of floodwater is repeatedly forced out of the channel, salmon swimming upstream to spawn are stranded on the floodplain (U.S. Army Corps of Engineers (USACOE), 2014). While it is generally accepted that flooding has resulted from a reduction in the channel's bankfull channel capacity due to sediment accumulating in the channel (Jay and Simenstad, 1996; Stover and Montgomery, 2001; Bountry et al., 2009; USACOE, 2014), the cause or causes of the channel capacity loss has not been systematically examined. Although much effort and funding has been expended to improve habitat or

* Corresponding author.
E-mail address: bcollins@uw.edu (B.D. Collins).
[1] Present address: Natural Systems Design, 1900 Northlake Way Suite 211, Seattle, WA 98103, USA.
[2] Present address: Department of Earth and Atmospheric Sciences, Indiana University, Bloomington, IN, 47405, USA.
[3] Present address: PanGEO, 3213 Eastlake Ave. E, Suite B, Seattle, WA 98102, USA.

https://doi.org/10.1016/j.geomorph.2019.01.021
0169-555X/

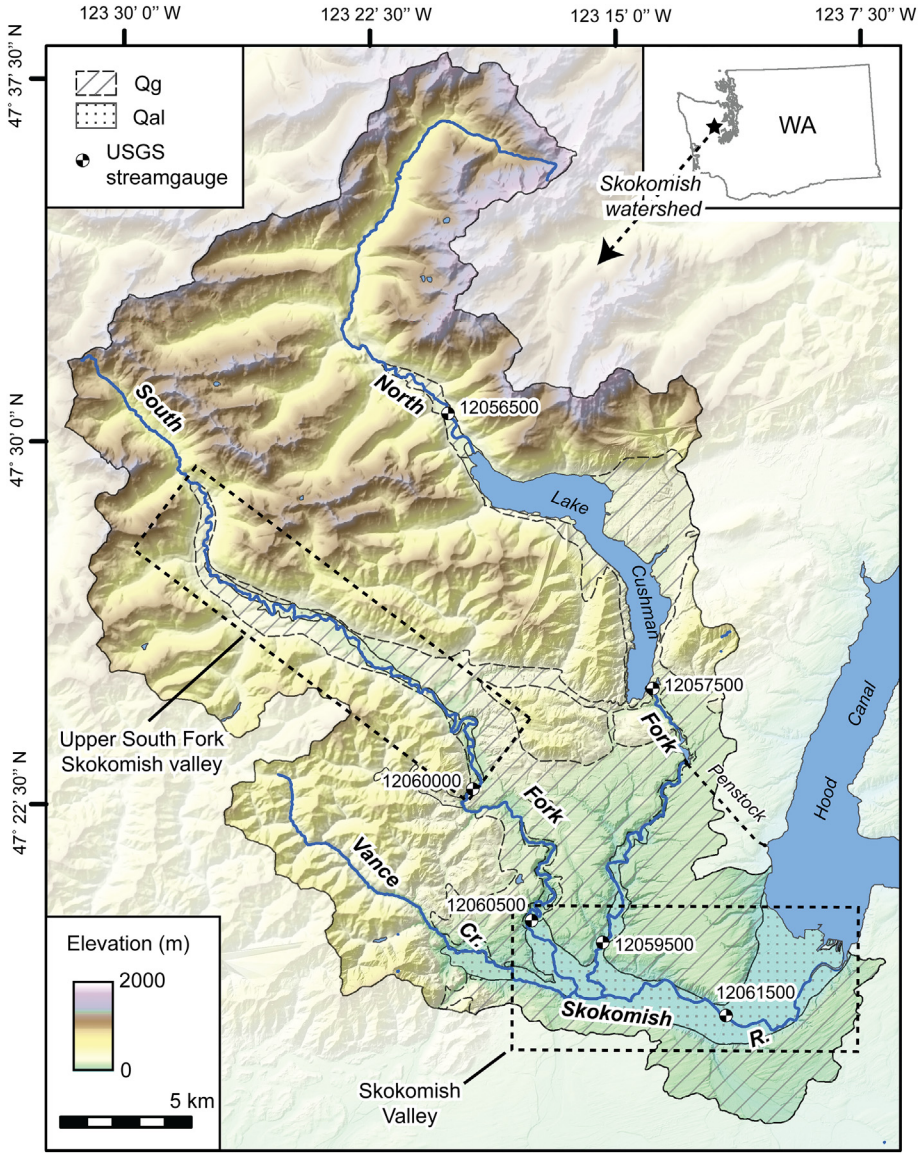

Fig. 1. Topography of the Skokomish River watershed in Washington State. Hatching shows extent of Pleistocene glacial drift (Qg) and stippled pattern shows Holocene alluvium (Qal), generalized from Logan (2003).

mitigate flooding, a lack of clarity about the cause(s) of capacity loss inhibits effective planning to remedy or adapt to the problem.

The river's two forks have different geologic and human histories and feature in two different hypotheses that have been advanced to explain flooding in the mainstem. The North Fork, draining 304 km^2 and heading in Olympic National Park, has been impounded and diverted out of basin by the Cushman Hydroelectric Project since 1930 (U.S. Department of Energy (USDOE), 2010). The Cushman Project consists of two dams, 14 and 17 river kilometers (rkm) upstream of the North Fork's confluence with the South Fork. Cushman No. 2, the lower of the two dams, transfers water out of the Skokomish basin to a powerhouse on the Hood Canal (Fig. 1), substantially reducing flood peaks in the mainstem. This flow reduction has been invoked to explain at least part of the conveyance loss (Jay and Simenstad, 1996; Stover and Montgomery, 2001; Bountry et al., 2011). The South Fork basin, draining 205 km^2 (269 km^2 inclusive of the Vance Creek basin; Fig. 1) and owned by private timber companies and the U.S. Forest Service, has not been dammed, but experienced extensive timber harvesting in the second half of the twentieth century, and erosion associated with timber harvesting has been invoked to explain part (Jay and Simenstad, 1996; Stover and Montgomery, 2001) or all (Simons and Simons, 1997; Curran, 2016) of the downstream capacity loss. Along the mainstem, levees built in the last third of the twentieth century to manage flooding have been speculated to be a third potential cause of sedimentation and channel conveyance loss (Bountry et al., 2009; Curran, 2016).

While understanding the causes and persistence of flooding in the Skokomish River is an important regional issue, it also exemplifies several broader concerns: First, in assessing or predicting flood risk, there is often the need to differentiate between changes to channel capacity and changes to streamflow (Slater et al., 2015) and whether changes to channel capacity, in turn, may be caused by climate change (Slater and Singer, 2013), land use, or river engineering. Second, planning for development or removal of hydropower dams must be informed by an understanding of potential downstream impacts. Whereas a number of case studies on the downstream effects of dams (see Grant, 2012, for review) provide a basis for predictive models of channel response (Grant et al., 2003; Schmidt and Wilcock, 2008; Curtis et al., 2010), relatively few studies have placed dams within a broader context of multiple watershed drivers to channel change (Grant, 2012). Finally, this study illustrates how geomorphic evidence can be used to determine the causes and potential solutions to flooding in a river system having multiple natural and anthropogenic influences on sedimentation and flooding. To systematically evaluate several hypotheses on the causes

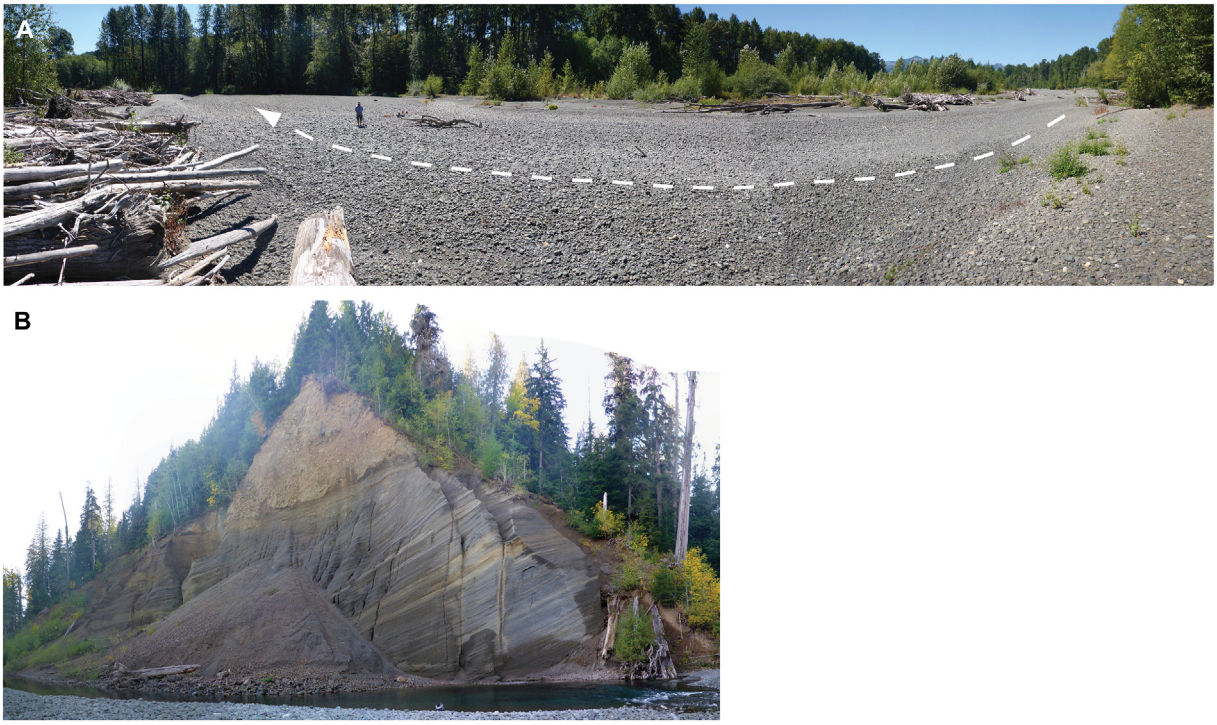

Fig. 2. (A) Dewatered reach of the Skokomish River (see Fig. 4B) in August 2016; arrow shows flow from right to left. (B) Eroding face of terrace formed in unconsolidated glacial sediments in the upper South Fork River at South Fork rkm 29. Maximum bluff height is 60 m; flow is from right to left.

of flooding in the Skokomish River, we evaluate historic change to: (1) channel morphology, (2) bed elevation, (3) peak streamflow, and (4) sediment inputs and yield.

2. Study area

2.1. Geology and topography

The transport of sediment from most of the North Fork's basin downstream to the mainstem was limited historically by the presence of the natural, moraine-dammed Lake Cushman (Bretz, 1913), which the Cushman hydroelectric project enlarged (Fig. 1). While the natural Lake Cushman was smaller than the modern reservoir, historical maps (e.g., U.S. General Land Office, 1878; Jones, 1925) and early descriptions (e.g., by the 1890 O'Neil Expedition, in Wood, 1976, pp. 69–70) show the historical lake was large enough to have functioned as an effective sediment sink for coarse sediment, with a surface area in the late 1800s of about 2 km^2 (U.S. General Land Office, 1878, 1893). Because 82% (248 km^2) of the 304 km^2 of the North Fork basin drained into historical Lake Cushman, the sediment load of the North Fork at its confluence with the South Fork would historically have been lower than that of the South Fork, which drains a 269 km^2 basin.

The upper South Fork flows through a glaciated valley having steep valley slopes and a broad valley bottom (Fig. 1) and is forested except at the highest elevations. The gradient of the South Fork (Fig. 3A) declines from its steep headwaters to a moderate gradient (0.004–0.02) in the upper, glacier-carved valley, where the river is flanked by alluvial terraces consisting of unconsolidated sediments (Fig. 2B) from alpine and continental glaciations (Dragovich et al., 2002). A previous study (Washington State Department of Natural Resources (WADNR), 1997b) inferred that lateral stream erosion of these terraces is the dominant source of sediment to the upper South Fork. Elsewhere in the region where extensive Pleistocene glacial deposits fill valley bottoms, remobilization of these sediments, or "paraglacial sedimentation" (Church and Ryder, 1972), can dominate basin sediment yields (e.g., Church and Slaymaker, 1989), and may explain why sediment yield from the Skokomish watershed is high relative to comparable non-glacierized Puget Sound basins (Czuba et al., 2011).

Downstream of the upper valley, the South Fork descends through a generally steep (Fig. 3B), confined bedrock gorge (Fig. 1) carved into the basaltic Crescent Formation (Dragovich et al., 2002) before entering the lowland Skokomish Valley (Fig. 1). This lowland valley, likely created by sub-glacial runoff in the late stages of the Fraser glaciation (Booth, 1994), is broad (2–3 km wide) and has a low gradient (0.002). On entering the lowland Skokomish Valley, the South Fork downstream of the gorge and above the confluence with the North Fork (referred to here as the "lower South Fork;" Fig. 1) has an average channel gradient of 0.0025 (Fig. 3C). Only three river kilometers downstream of its gorge, the South Fork joins the North Fork, which has built an extensive Holocene alluvial fan into the Skokomish Valley. Downstream of this confluence, the Skokomish River's channel gradient declines by a factor of two, to 0.0013 (Fig. 3C).

The South Fork has built a valley-wide depositional ramp (Figs. 4 and 5A) into the Skokomish River valley; downstream of the confluence of the North and South forks this ramp narrows to an alluvial ridge up to 3 m higher than the flood basins that flank the river (Fig. 5B-D). This valley-bottom morphology is similar to that formed by rivers in the eastern Puget Sound lowland also flowing in troughs carved by sub-glacial runoff (Collins and Montgomery, 2011) and causes flooding to be deep and persistent; the original public land survey maps and field notes describe extensive backswamps in the valley's flood basins (U.S. General Land Office, 1861).

Because of a progressive increase to the channel's bed elevation in the last half century, the channel of the North Fork avulsed in about 2004 (Fig. 4) from its historic location, and has since flowed downvalley parallel to the Skokomish River, in the topographic low between the North Fork's Holocene fan to the north and the Skokomish River's alluvial ridge to the south (Fig. 5B), for two river kilometers before a valley-bounding glacial terrace forces it to join the Skokomish River (Fig. 4).

The Skokomish Valley is a natural depositional reach, but existing estimates indicate that recent deposition rates recorded at a stream gauge

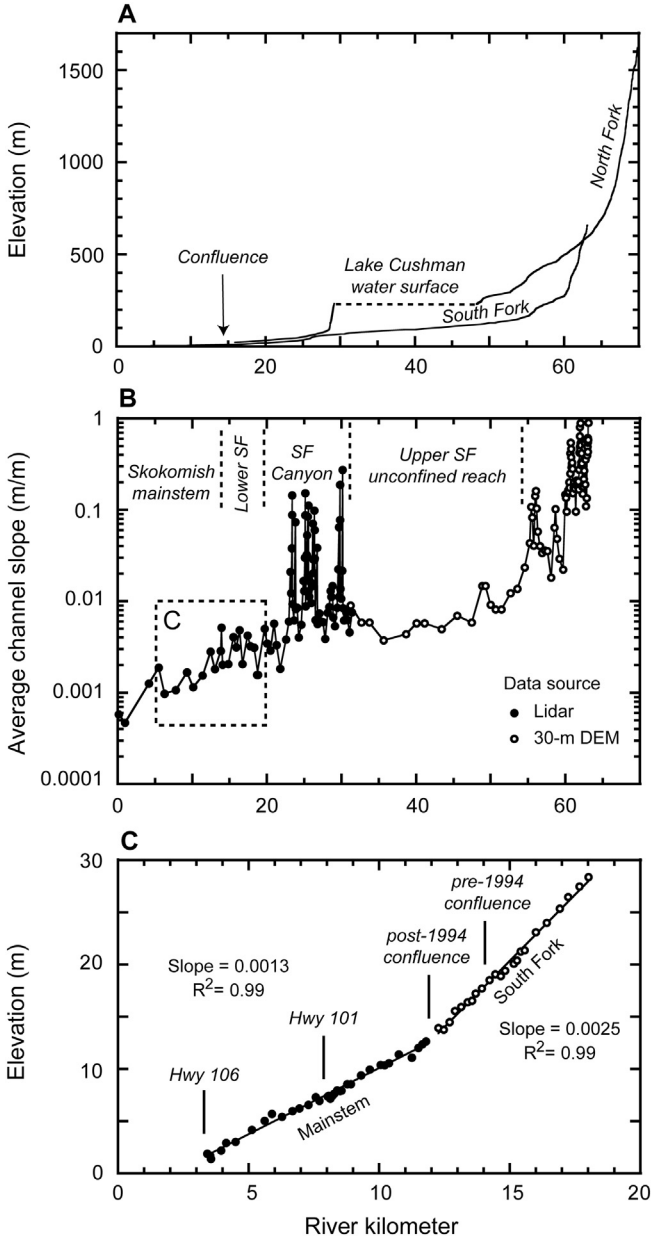

Fig. 3. (A) Longitudinal profile of the Skokomish River and forks, from 30-m digital elevation model (DEM). (B) Channel slope of the Skokomish and South Fork Skokomish rivers, from lidar and 30-m DEM. (C) Slope of the Skokomish River mainstem and lower South Fork Skokomish River, from average bed elevations measured by cross sections surveyed in 2007.

(Stover and Montgomery, 2001) are greater than late Holocene rates implied by radiocarbon dating (Bountry et al., 2009). Because the valley is only about 10 km in length, the entire coarse sediment load from the two forks deposits in a relatively short distance before the river reaches sea level at the Hood Canal (Fig. 1). Regional sea level rise over the last 1000 yr has been <1 m (Eronen et al., 1987; Beale, 1990). There was at least 1 m of likely co-seismic uplift and tilting at the delta front about 1000 yr ago; this has had the effect of maintaining the river's position near to the valley's south wall in the lower-most three river kilometers (Arcos, 2012). Stratigraphic descriptions by Bountry et al. (2009) indicate the river has occupied the same general part of its valley for the last 500–2000 yr (Bountry et al., 2009, p. 40) during which time sedimentation rates, indicated by 11 radiocarbon dates, averaged 0.002 m yr^{-1} (Table C-1 in Bountry et al., 2009). In contrast, rates of vertical sediment accumulation in the active channel in the last half century has averaged about 0.03 m yr^{-1} (Stover and Montgomery, 2001), >10 times the late-Holocene valley sedimentation rates implied by the radiocarbon dates from Bountry et al. (2009).

2.2. History of forest cutting

Logging proceeded up-valley in three phases, beginning in the last three decades of the nineteenth century. While the Skokomish Valley's first logging camp was established in 1887 “six miles upriver” (Richert, 1984), the progress of logging farther up-valley was limited by river-filling log jams that prevented downstream log transport (U.S. General Land Office, 1861; Richert, 1984). River-filling jams appear to have been removed by 1892 (Richert, 1984), and federal land cover mapping (Rankine and Plummer, 1898; Plummer et al., 1902) shows that by 1898 logging and conversion of the valley to farming had proceeded up-river to within 1 km of the South Fork gorge and 2.5 km up the Vance Creek valley. The first aerial photos show that, by 1929, logging had been limited to the valley sides of the Skokomish Valley and to a patch in the southwest corner of lower Vance Creek where railroad logging had recently entered the watershed from the west (Fig. 6B). A second wave of logging from the last years of the 1930s through the 1940s used tractor-logging techniques on the gently- to moderately-sloping terrain in the lower part of both forks (Figs. 1 and 6C). A third wave of logging, in the last four decades of the twentieth century, extended into the steeper upper South Fork and Vance Creek watersheds, primarily on U.S. Forest Service land (Fig. 6D–E), and used cable-logging techniques along an extensive network of roads. Most logging in the most recent two decades has been of lower-elevation second growth forest first cut in the 1930s and 1940s (Fig. 6F).

2.3. Cushman hydroelectric project

Cushman No. 1 was completed in October 1925 (Perrin et al., 2014) at which time the Cushman Reservoir began to fill and downstream flow regulation began (U.S. Geological Survey (USGS) streamflow gauging station 12057500); a second, downstream dam, Cushman No. 2, was completed in 1930 (USDOE, 2010). Cushman No. 1 generates power in a powerhouse located about 200 m downstream of the dam, while Cushman No. 2 withdraws water from the North Fork through a penstock to a generating facility on Hood Canal (Fig. 1). Prior to 1988, the project diverted between 35 and 42% of the total annual flow of the Skokomish basin (USDOE, 2010). An instream flow requirement of 0.8 $m^3\ s^{-1}$ (30 $ft^3\ s^{-1}$) was instituted in July 1988 (USDOE, 2010) and increased to 6.8 $m^3\ s^{-1}$ (240 $ft^3\ s^{-1}$) in 2008 (USDOE, 2009). Prior to 1988, flow in the North Fork immediately downstream of the Cushman Project was limited to seepage or spill during floods or project maintenance.

2.4. History of river engineering

Local interests, with federal support, primarily in the 1930s, used wing dams and revetments to prevent bank erosion at several locations in the mainstem (WA Dept. of Conservation and Development, 1935; Dunn, 1941). Notes by USGS stream gauging personnel indicate that the Washington Department of Highways removed gravel in the early 1930s from the lower Skokomish River. Federal agencies (Dunn, 1941) straightened the channel at rkm 6, bracketed by aerial photos to between 1938 and 1940, by eliminating two adjacent meanders (Fig. 4A). Finally, mapping by the Bureau of Reclamation (Bountry et al., 2009) and aerial photos indicate that 5 km of discontinuous levees were later constructed in the eight river kilometers downstream of the North Fork confluence (Fig. 4B).

3. Approach

To assess capacity loss in the Skokomish River, we characterized temporal change to the channel capacity by: mapping the channel

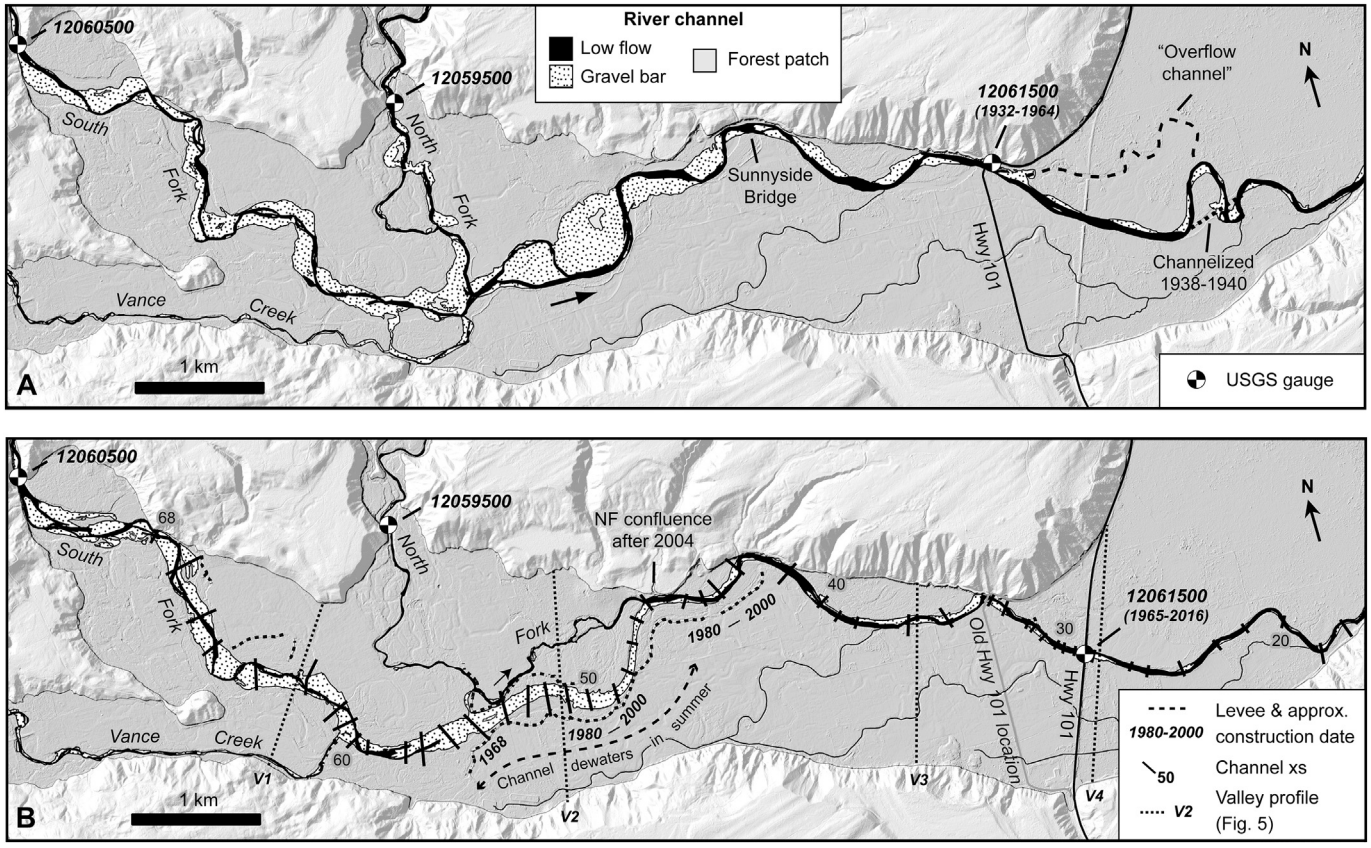

Fig. 4. The Skokomish Valley, 1938 and 2015. (A) The 1938 active channel (gravel bars and low flow channel) and forest patches digitized from aerial photos. Downstream of the Highway 101 bridge dashed line shows channel identified as "overflow channel" on a 1935 map (Washington Dept. of Conservation and Development, 1935) and two channel meanders cutoff between 1938 and 1940. (B) The 2015 active channel and location of levees and their approximate dates of construction, and locations of channel cross sections surveyed in 1994, 2007, and 2016 (Fig. 10), valley cross sections from lidar (Fig. 5), and portion of the channel that typically dewaters in summer.

planform from maps and aerial imagery from 1929 through 2015; surveying channel cross sections in 2016 at locations of cross sections that had been previously surveyed in 2007 and 1994; and characterizing changes to channel-bed elevation at USGS stream gauges. To evaluate the hypotheses that levee building along the mainstem or flow reduction from the Cushman Projects caused the capacity loss, we compared the timing of levee and dam building with the timing, magnitude, and spatial occurrence of capacity loss. To evaluate the hypothesis that capacity loss resulted from increased rates of sediment production from forestry or a systematic increase to peak flows, we: quantified sediment sources from an existing landslide inventory and from field- and photo-measured rates of stream erosion of alluvial terraces and floodplains; reconstructed the historical spatial extent and timing of forest harvest; examined stream gauging records for evidence of systematic change through time; and estimated the yield of sediment from the Skokomish River from analysis of existing suspended and bedload sediment measurements combined with our measurements of channel sediment storage change.

4. Methods

4.1. Peak flow history

Flood peaks in the Skokomish basin have been recorded at several gauges since 1914 but not continuously at any gauge (Table 1). Peak flows in the North Fork were measured at the upstream dam site (Cushman No. 1) in WY 1914–1929 (North Fork Skokomish River near Hoodsport, WA, USGS 12057500, herein referred to as "North Fork at Cushman No. 1"); within the period WY 1914–1925, flows were unaffected by flow regulation. Peak flows of the regulated North Fork were gauged at a site downstream of Cushman No. 2 and 2.3 rkm above the confluence (North Fork Skokomish River near Potlatch, WA, USGS 12059500, herein referred to as "lower North Fork") (Fig. 1). We estimated pre-regulation peak flows (1914–1925) at the lower North Fork gauge using flows at the North Fork at Cushman No. 1 gauge and the drainage area ratio method of Thomas et al. (1994) with an exponent of 0.98 from Knowles and Sumioka (2001). Upstream of the Cushman Projects and the natural Lake Cushman, unregulated peak flows in the North Fork were measured in WY 1925–2016 (North Fork Skokomish River below Staircase Rapids near Hoodsport, WA, USGS 12056500, herein referred to as "North Fork above Cushman"). We used these flows to estimate unregulated peak flows in the mainstem Skokomish, as described below.

The longest record on the South Fork (1932–1984 and 1996–2016) is from a gauge at the downstream end of the South Fork's gorge (South Fork Skokomish River near Union, USGS 12060500, herein referred to as "South Fork"). We used linear regression to estimate peak flows at the South Fork gauge for the WY 1985–1995 period from the Skokomish River near Potlatch gauge (USGS 12061500, herein referred to as the "mainstem" gauge) and for 1924–1931 from an upstream gauge on the South Fork (South Fork Skokomish River near Potlatch, WA, USGS 12060000, herein referred to as the "upper South Fork"), which was gauged in WY 1924–1932 and WY 1947–1964.

Gauging of the mainstem Skokomish River did not begin until 1944, after the Cushman Project was completed. Since WY 2010, the USGS has not gauged flows greater than about 110–140 $m^3\ s^{-1}$ (4000–5000 $ft^3\ s^{-1}$) because the river overflows its banks upstream into several channels that bypass the gauge; we estimated missing daily flows for the WY 1995–2016 period by a regression of flows at the mainstem gauge with combined flows from the South Fork and North Fork gauges

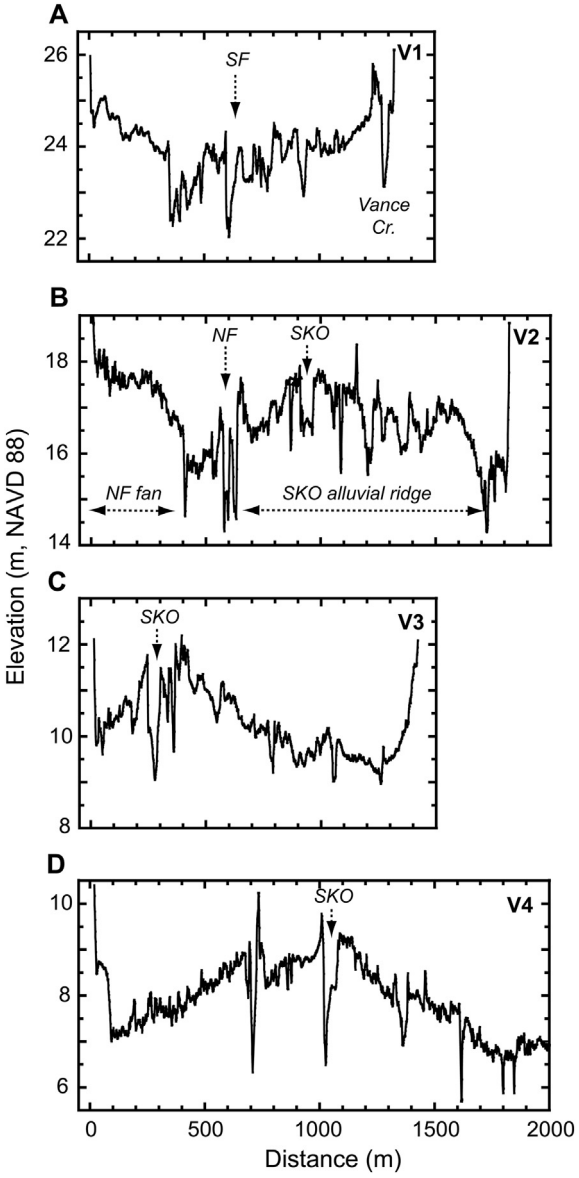

Fig. 5. Topographic profiles, from water-penetrating 2015 lidar, across the Skokomish River valley at four representative locations shown in Fig. 4. Profiles are from left to right, looking down valley (north to south). Labels and arrows are locations of the channels of the South Fork Skokomish ("SF"), North Fork ("NF"), Skokomish ("SKO"), and Vance Creek.

($Q_{mainstem} = 1.00\ (Q_{NF} + Q_{SF})^{1.10}$, $R^2 = 0.97$, $N = 2661$). We estimated peak flows for WY 1932–1933 and 1935–1943 from the South Fork gauge. For both the South Fork and mainstem gauges, we fit the recorded peak annual floods to a Log Pearson Type-III frequency distribution.

We took two approaches to estimating the unregulated magnitude and frequency of floods at the mainstem gauge. For the pre-regulation period (i.e., 1914–1925), we used the drainage-area ratio approach to scale flows for the South Fork from the South Fork gauge and for the North Fork from the North Fork Cushman No.1 gauge. Because this approach is limited to the brief pre-regulation record at the North Fork at Cushman No. 1 gauge, we also estimated unregulated peak flows (i.e., post-1925) by scaling flows from the North Fork above Cushman gauge and the South Fork gauge. The robustness of this second approach is limited by the need to determine an empirical flood peak attenuation factor, to account for the effects of historical Lake Cushman, from the single year of overlap between the unregulated record at the Cushman No. 1 gauge and the North Fork above Cushman gauge; we determined an attenuation factor of 0.83 from two flood peaks in WY 1925 by using the area-ratio approach to predict flows at the Cushman No. 1 gauge from the gauge above Cushman and comparing the predicted and observed flows at the Cushman No. 1 gauge.

4.2. Historical change in bankfull channel capacity

To quantify how the bankfull channel capacity has changed through time, we concentrated on the mainstem gauge, which has the most extensive record. The gauge is in a straight reach (Fig. 4B) and the channel at the gauge has an uncomplicated trapezoidal cross-sectional shape. We relied primarily on field observations by USGS stream gauging personnel of the stage and discharge at which water began to overflow the banks, or, on one occasion (12/2/1941), the stage at which water was overflowing the banks, as recorded on field measurement forms (USGS form 9–275). We also used field discharge measurements, grouped by decade, to plot the width-to-depth ratio against the average flow depth, fit a parabola to the data and took the vertex (minima) as the bankfull depth (e.g., Knighton, 1998, Fig. 5.6B), and convert this flow depth to a discharge by creating a stage-discharge rating curve for that decade; overbank flows were only frequent enough to confidently determine this value for the last three decades of the record. We supplemented these two indicators of bankfull capacity with published measurements of bankfull discharge by the USACOE (Dunn, 1941) and US Geological Survey (Cummans, 1973) and estimates from hydraulic models (KCM, 1997; Bountry et al., 2011).

4.3. Streambed elevation change at USGS stream gauges

We used USGS stream gauging records to characterize annual changes to bed elevation by determining the water surface elevation at a given discharge, an approach that has been applied to a range of applications in the last century (e.g., Gilbert, 1917; Williams and Wolman, 1984; Collins and Dunne, 1989; James, 1991, 1997; Juracek, 2000; Pinter et al., 2000; Pinter and Heine, 2005). We used this approach, rather than directly determining the bed elevation by averaging bed elevations from each discharge measurement (e.g., Stover and Montgomery, 2001) or by approximating the bed elevation by dividing the cross-sectional area for each discharge measurement by the stream width and subtracting the flow depth from gauge height (e.g., Slater and Singer, 2013) because the water surface elevation, as a hydraulically-smoothed representation of bed elevation, should be a better indicator of the reach-averaged, rather than local, bed elevation.

We obtained discharge measurement summary sheets (USGS form 9–207) and discharge measurement notes (USGS form 9–275) from the US Geological Survey for the period of record for five gauges (Table 1). For each water year, we created a rating between discharge and gauge height and determined the gauge height for the median discharge for the period of record (e.g., Czuba et al., 2010); we did this rather than computing the difference between individual measurements and a single stage-discharge rating (e.g., James, 1991) to focus on change at the annual and decadal rather than monthly scale. The mainstem gauge was moved 1 rkm downstream to its current location in 1965 (Fig. 4B); because measurements were made at both stations in 1964 it was possible to correlate elevations at the upstream station to the datum of the current location.

4.4. Channel cross-sectional change

To characterize rates and spatial patterns of bed elevation change in the Skokomish and lower South Fork Skokomish rivers, in summer 2016 we resurveyed cross sections originally surveyed for a flood study in 1994 (KCM, 1997) and resurveyed for a subsequent flood study in 2007 (Tetra-Tech, 2007) (Fig. 4B). The 2007 survey points were provided as northing and easting coordinates in GIS shape files by the US Bureau of Reclamation (Jennifer Bountry, email communication, 2016). The 1994 survey data were provided as distances and elevations without

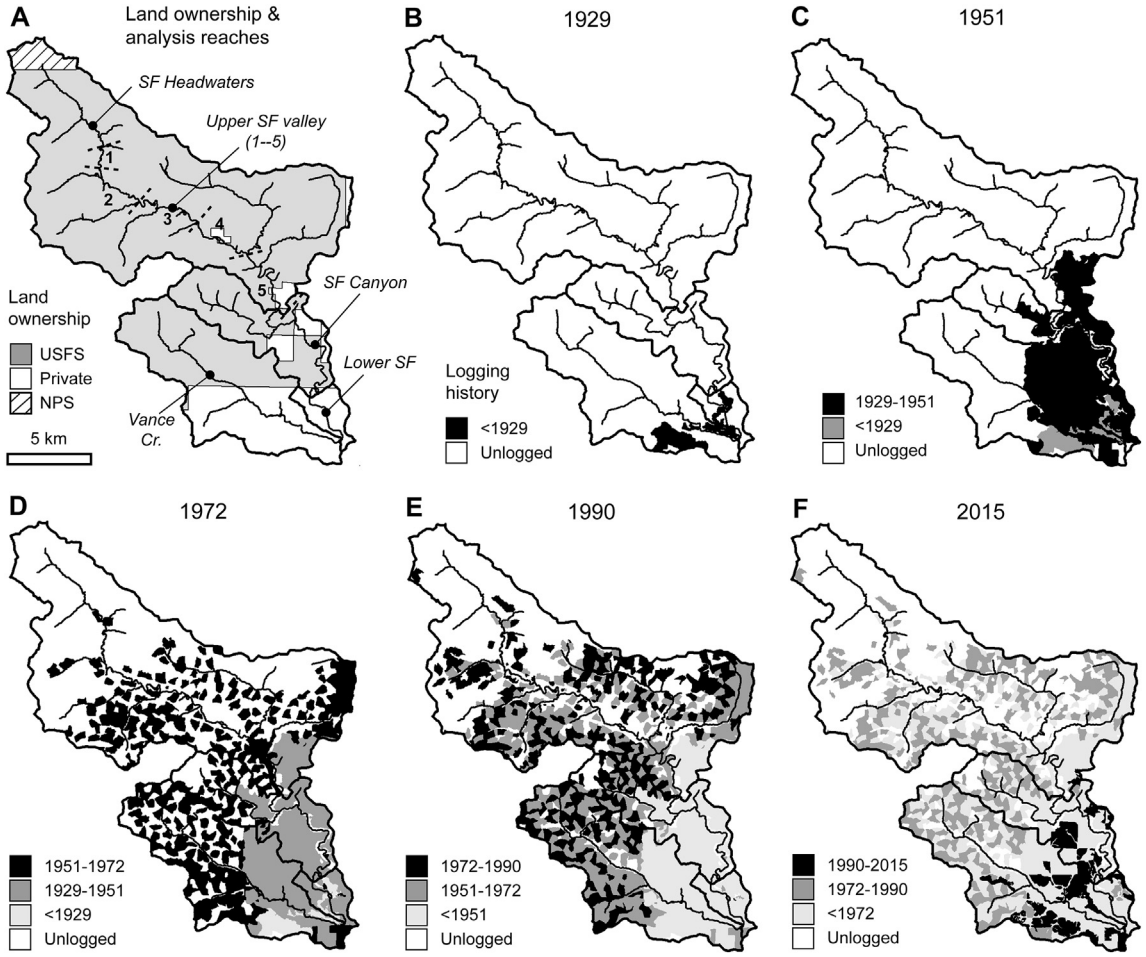

Fig. 6. Land ownership and history of forest clearing in the South Fork Skokomish watershed. (A) Numbered reaches, demarcated by dashed lines, refer to channel segments in the upper South Fork valley in Fig. 13. (B)–(F) Logging history, showing status of forest in 1929, 1951, 1972, 1990, and 2015. Data compiled from USFS 2015 stand age mapping (U.S. Forest Service, 2016) and from interpretation of aerial photos (Table 2).

georeferenced endpoints in a spreadsheet by the US Army Corps of Engineers (Karl Eriksen, email communication, 2014).

We surveyed 36 of the 42 cross sections upstream of the Highway 101 bridge; in the kilometer upstream of Highway 101 we reoccupied every other cross section because cross sections in that reach were more closely spaced than elsewhere. We reoccupied the 2007 cross sections using a Trimble R10 GPS and the Washington State Reference Network to locate two 2007 survey points along each cross section; the mean vertical precision of these initial points was 7.8 mm (0.026 ft) (standard deviation = 2.4 mm (0.012 ft); minimum = 4.3 mm (0.014 ft), maximum = 17.7 mm (0.058 ft)). We then used a total station to survey the cross section along the line established by the two reoccupied points. Residuals associated with total station set up (i.e., the difference between the elevation of the second point measured by GPS and the elevation of the second point measured by the total station) averaged −0.3 mm (−0.001 ft) (standard deviation = 15.2 mm (0.050 ft)). Summing the GPS precision and station set up precision indicates the vertical precision of the 2016 cross sections was generally <1 cm, and in all cases <2 cm.

Cross sections were not spaced at equal distances throughout the reach, with an average spacing of 0.26 km between cross sections in the 7.4 km from the Highway 101 bridge to Vance Creek and 0.51 km in the 4.1 km between Vance Creek and the South Fork gauge, with a spacing of 0.8 km in the upper 2.4 km of the latter reach. To account for the difference in spacing, we averaged cross-sectional change in each sub-reach and multiplied that average by the distance of the

Table 1
USGS gauges in the Skokomish River watershed used in this analysis.

Gauge number	Gauge name	Name used in this paper	River km[a]	Drainage area (km^2)	Peak flow period of record (WY)
12061500	Skokomish River near Potlatch, WA	"mainstem"	8.5	588	1934, 1943–2016
12060500	South Fork Skokomish River near Union, WA	"South Fork"	SF 5	198	1931–1984, 1996–2016
12060000	South Fork Skokomish River near Potlatch, WA	"Upper South Fork"	SF 15	170	1924–1932, 1947–1964
12059500	North Fork Skokomish River near Potlatch, WA	"lower North Fork"	16.1	303	1945–2016
12057500	North Fork Skokomish River near Hoodsport, WA	"North Fork at Cushman No. 1"	32	243	1914–1925
12056500	North Fork Skokomish River below Staircase Rapids near Hoodsport, WA	"North Fork above Cushman"	46.9	148	1925–2016

[a] River kilometers are from USGS topographic maps and are continuous along the mainstem and North Fork or along the South Fork ("SF") starting at its confluence with the North Fork.

reach to determine volumetric change for that sub-reach; similarly, to compute average elevation change, we spatially-weighted the average elevation change by sub-reach length.

4.5. Channel planform change in the lower South Fork and Skokomish mainstem

To characterize change through time to the channel planform of the lower South Fork and the mainstem, we digitized aerial imagery from 1929 to 2015 including georeferenced digital imagery, from 1990 through 2015, and aerial photographs, from 1929 through 1985, that we scanned and georeferenced or orthorectified (Table 2). On each set of images, we digitized the low-flow channel, gravel bars, and forest patches having a closed canopy; we took the combined low-flow channel and gravel-bar areas as the active channel area. Because photographs were taken in low-flow months of June through September and because we analyzed the active channel, it was not necessary to control for differences in streamflow between photos. To characterize channel width, we used a GIS to generate a series of transects orthogonal to a generalized active-channel centerline (Legg et al., 2014) for the 1929–2015 period, spaced at 200-m intervals, and to measure the length of each transect intersecting the active channel for each imagery year. We bracketed the date of construction of streamside levees from GIS data provided by the U.S. Bureau of Reclamation (Jennifer Bountry, email communication, 2016) supplemented with aerial photo analysis.

4.6. Channel planform change and sediment production in the upper South Fork

In the upper South Fork basin, we measured channel planform area and width as described above. To estimate sediment influx from alluvial terraces, in September 2017 we mapped channel-adjacent bluffs and their heights; to determine volumetric erosion of bluffs alone (i.e., excluding floodplain erosion), we measured areal change along field-identified bluffs in the period between the first reliably-georeferenced imagery from 1990/1994, and 2015 (Table 2). To convert this volume to a mass, we derived an average bulk density of 2000 kg m^{-3} by visually estimating the relative thickness of the two units exposed in bluffs, glacial outwash and glacial till, and multiplying the proportion of each unit by the bulk density for each unit. We used bulk density values from elsewhere in western Washington of 1910 kg m^{-3} for Vashon outwash (Savage et al., 2000) and 2250 kg m^{-3} for Vashon Till (Easterbrook, 1964; Savage et al., 2000). To determine sediment influx from erosion of floodplains, we combined the photo-determined lateral channel migration with streambank heights field-measured in 2013, 2014, and 2017, from which we derived an average bank height of 2.5 m.

We used a previous landslide inventory by the State of Washington (WADNR, 1997a) to characterize the timing, location and quantity of landsliding. To convert volumetric sediment delivery rates reported in WADNR (1997a) to mass, we assumed an average bulk density for colluvium of 1600 kg m^{-3} from six samples of colluvium gathered at three sites in the Olympic Peninsula by Schroeder and Alto (1983). To assess the possibility that riparian logging promoted channel widening, we mapped logging history in the South Fork basin from aerial photographs and a 2015 forest stand-age map created by the U.S. Forest Service (U.S. Forest Service, 2016).

To compare the timing and magnitude of sediment sources from the Skokomish basin to flux through the Skokomish River at the Highway 101 bridge, we estimated the suspended and bedload sediment loads of the Skokomish River at the USGS gauge at Highway 101. We created a rating curve for suspended sediment by combining field measurements by the USGS (WY 1996–1998, 2010) with field measurements in WY 1993–1994 by Simons & Associates (1994) and applying a bias correction factor (BCF) (Duan, 1983); the resulting relation between daily discharge, Q ($m^3\ s^{-1}$), and daily suspended sediment discharge, Q_s (Mg d^{-1}) is $Q_s = 0.00375\ Q^{2.62}$ BCF ($R^2 = 0.89$), where BCF = 1.64. We created a rating curve for bedload transport by combining samples from the USGS (nine measurements in WY 2010–2011) with measurements by Simons & Associates (17 measurements in WY 1993–1994); the resulting ratings between daily discharge, Q ($m^3\ s^{-1}$), and daily bedload flux, Q_b (Mg d^{-1}), are, for $Q \geq 49\ m^3\ s^{-1}$, $Q_b = 2.32$ E-3 $Q^{2.52}$ BCF ($R^2 = 0.63$) where BCF = 1.36, and, for $Q < 49\ m^3\ s^{-1}$, $Q_b = 5.45$E-18 $Q^{11.4}$. We applied the suspended and bedload sediment ratings to daily flows for the period of record at the gauge, WY 1944–2017, estimating missing high flows as described previously. Our calculated suspended sediment flux agreed within 1% of an estimate by Grossman et al. (2015) made from USGS samples alone; our calculated bedload was 24% less than that made by Grossman et al. (2015) from USGS data alone. While including the Simons & Associates data nearly tripled the number of bedload samples in our rating compared to using USGS data alone, the estimate nonetheless has large uncertainty because none of the measurements were made at flows larger than 295 $m^3\ s^{-1}$ (10,400 $ft^3\ s^{-1}$), none of the USGS measurements were from flows larger than 194 $m^3\ s^{-1}$ (6840 $ft^3\ s^{-1}$), and more than half (54%) of the bedload calculated to have transported over the period of record was in the 0.8% of days with a flow exceeding 280 $m^3\ s^{-1}$ (10,000 $ft^3\ s^{-1}$).

Table 2
Aerial photographs and satellite imagery used in channel planform change analysis. Imagery type abbreviations: B&W: black and white; SFP: single frame photo; DOQ: digital orthophoto.

Year of imagery	Scale or resolution	Type	Originating agency or firm	Source
1929	1:14,400	B&W SFP	Fairchild Aerial Surveys	1
1938	1:10,000	B&W SFP	USACOE	3
1939	1:30,000	B&W SFP	USGS	4, 6
1942	1:20,000	B&W photomosaic	USACOE	2
1946	1:14,400	B&W SFP	Fairchild Aerial Surveys	5
1951	1:37,400	B&W SFP	USGS	6
1957	1:12,000	B&W SFP	Wash. State Dept. of Transportation	2
1962	1:12,000	B&W SFP	USDA Forest Service	2
1968	1:80,000	B&W SFP	USGS	6
1972	1:70,000	B&W SFP	USDA Forest Service	2
1980	1:80,000	B&W SFP	USDA Forest Service	2
1985	1:24,000	Color SFP	USGS	6
1990	1 m	B&W DOQ	USGS	6
1994	1 m	B&W DOQ	USGS	6
2004	2 m	Color digital	USDA NAIP	7
2005	2 m	Color digital	USDA NAIP	7
2006	1 m	Color digital	USDA NAIP	7
2009	1 m	Color digital	USDA NAIP	7
2011	1 m	Color digital	USDA NAIP	7
2013	1 m	Color digital	USDA NAIP	7
2015	1 m	Color digital	USDA NAIP	7

1 University of California Santa Barbara Libraries, Santa Barbara, WA (http://www.library.ucsb.edu/map-imagery-lab/collections-aerial-photography).
2 University of Washington Libraries, Seattle, WA.
3 Seattle District, Army Corps of Engineers, orthorectified by Puget Sound River History Project (http://riverhistory.ess.washington.edu/index.html).
4 U.S. Department of Agriculture, Olympic National Forest, Olympia, WA.
5 Green Diamond Resource Company, Shelton, WA.
6 USGS Earth Explorer (http://earthexplorer.usgs.gov/).
7 U.S. Department of Agriculture, National Agricultural Imagery Program.

5. Results

5.1. Peak flow history and effects of flow regulation on flood peaks

Peak annual floods at the South Fork gauge range from 242 $m^3\ s^{-1}$ (8550 $ft^3\ s^{-1}$) for the 1.25-yr flood to 711 $m^3\ s^{-1}$ (25,100 $ft^3\ s^{-1}$) for the 100-yr flood, and at the mainstem gauge range from 351 $m^3\ s^{-1}$ (12,400 $ft^3\ s^{-1}$) for the 1.25-yr flood to 931 $m^3\ s^{-1}$ (32,900 $ft^3\ s^{-1}$) for the 100-yr flood (Table 3). The two largest annual peaks of record

Table 3
Annual peak discharge frequency estimates, determined by fitting to a Log-Pearson III distribution, for (a) the pre-regulation North Fork Skokomish near Hoodsport gauge, USGS 12057500 ("North Fork at Cushman No. 1") from WY 1914–1925; (b) column a scaled to the drainage area of North Fork near Potlatch, USGS 12059500 ("lower North Fork"); (c) post-regulation flows at the lower North Fork gauge, WY 1944–2016; (d) North Fork below Staircase Rapids, USGS 12056500, WY 1925–2016; (e) the South Fork near Union ("South Fork"), USGS 12060500, WY 1932–1984 and 1996–2015; (f) the Skokomish River near Potlatch, USGS 12061500 ("mainstem"), WY 1933 and WY 1944-WY 2016; (g) pre-regulation mainstem estimated from columns a and e and (h) estimated from columns d and e; see text for detail on methods.

	Peak discharge ($m^3 s^{-1}$)							
	North Fork pre-regulation	North Fork regulated		South Fork	Mainstem regulated	Mainstem estimated pre-regulation	
Return period (yr)	(a) 12057500 North Fork near Hoodsport ("North Fork at Cushman No. 1")	(b) 12057500 (scaled to D.A. of 12059500 North Fork near Potlatch ("lower NF")	(c) 12059500 North Fork near Potlatch ("lower NF")	(d) 12056500 North Fork below Staircase Rapids (North Fork above Cushman")	(e) 12060500 South Fork near Union ("South Fork")	(f) 12061500, Skokomish River near Potlatch ("mainstem")	(g) estimated from 12057500 and 12060500	(h) estimate from 12056500 and 12060500
1.25	140	174	35.7	130	242	351	550	544
2	214	265	61.4	198	336	479	796	786
10	384	477	133	374	523	715	1320	1330
20	448	556	164	446	585	788	1500	1535
50	528	656	206	545	659	873	1730	1800
100	587	729	239	622	711	931	1900	2000

occurred in the 1990s (Fig. 7). Peak annual floods for the North Fork range from 35.7 $m^3 s^{-1}$ (1260 $ft^3 s^{-1}$) for the 1.25-yr flood to 239 $m^3 s^{-1}$ (8440 $ft^3 s^{-1}$) for the 100-yr flood. Peak annual flows in the South Fork have not increased systematically during the period of record; linear regression of peak flows for the period of record (1932–1984, 1996–2015) shows a weak, insignificant correlation. This result is unchanged by including one or both periods (1924–1931 and 1985–1995) of estimated peaks.

Comparing peak flows at the pre-regulation Cushman No. 1 gauge scaled up to the post-regulation lower North Fork gauge (Table 3) indicates that regulation reduced flows in the North Fork by an amount ranging from 79% for the 1.25-yr recurrence interval to 67% for the 100-yr flow. Using the brief peak flow record from the unregulated period at the Cushman No. 1 gauge and flows from the South Fork gauge to estimate the effects of regulation on flows at the mainstem gauge indicates that the reduction in flows from flow regulation ranged from 36% for the 1.25-yr recurrence interval flow to 51% for the 100-yr flow. Using the longer flow record from the North Fork gauge above Cushman with the South Fork gauge indicates similar reductions, ranging from 35% for the 1.25-yr recurrence interval flow to 53% for the 100-yr flow. While short records limit the robustness of both approaches (see Section 4.1), flows estimated by the two approaches agree within 1%

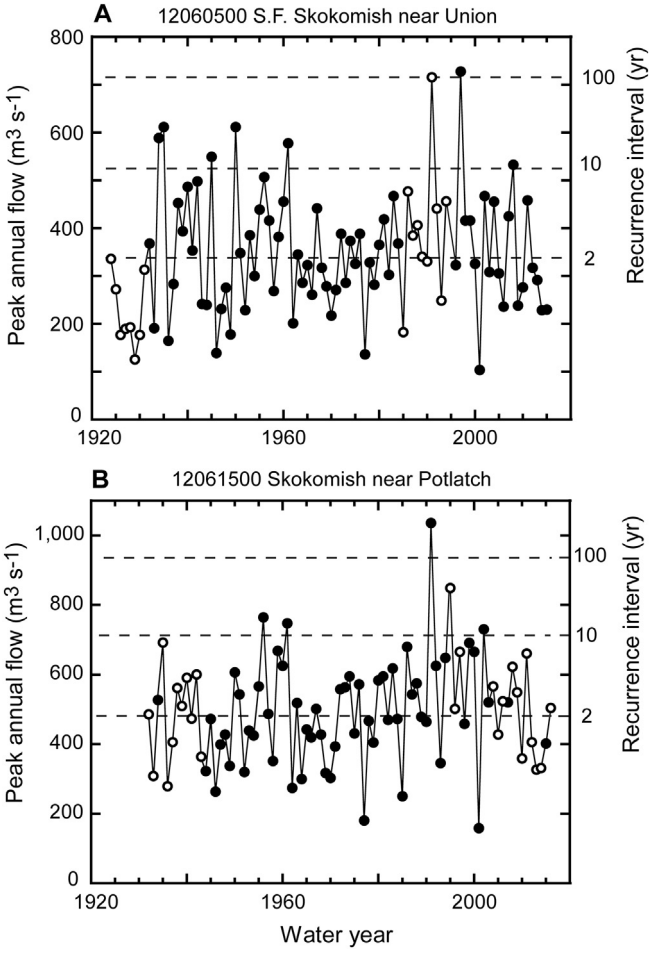

Fig. 7. Annual peak flows at (A) USGS gauge 12060500, South Fork Skokomish River at Union ("South Fork"). Missing peak flows (open symbols) were estimated for WY 1985–1995 from the mainstem Skokomish River gauge 12061500 and flows for WY 1924–1931 were estimated from the "upper South Fork" gauge 12060000. (B) USGS gauge 12061500, Skokomish River near Potlatch; peak flows for WY 1932–1933 and 1935–1943 were estimated from the South Fork (12016500) gauge, and missing peaks in the WY 1995–2016 period were estimated as described in the text. In both panels, the recurrence interval of the 2-yr, 10-yr, and 100-yr peak annual flood (dashed horizontal lines) was calculated from the period of record without including estimated flows (Tables 1 and 3).

for the 1.25-yr flow and within 5% for the 100-yr flow. Simons & Associates (1993) estimated that dam operations resulted in a reduction of 50% for a modeled 400 $m^3 s^{-1}$ (14,000 $ft^3 s^{-1}$) flow but do not indicate how they derived their estimate.

5.2. Timing and magnitude of historical loss to the Skokomish River's channel capacity

Bankfull channel capacity at the Highway 101 bridge gradually declined by a factor of about 4× since the first estimates made in an early flood control study by the USACOE (Dunn, 1941), which reported "the bankfull capacity of the Skokomish River channel is about 13,000 second-feet" (370 $m^3 s^{-1}$) (Fig. 8). This estimate appears to have been based on visual observations; Dunn (1941) indicates "flooding in valley begins at 13,000 cubic feet per second." Subsequent bankfull flow estimates in Fig. 8 include field observations made by USGS field personnel of the stage and discharge at which water began to overflow the banks, analysis of width-to-depth ratios from USGS gauging records, and a field study by Cummans (1973), who determined that in 1972 the channel could contain 250 $m^3 s^{-1}$ (8900 $ft^3 s^{-1}$) at the Highway 101 gauge (Fig. 8). The most recent estimates of bankfull channel capacity, indicated by width-to-depth ratios from USGS gauging records, are 80 and 85 $m^3 s^{-1}$; a U.S. Bureau of Reclamation hydraulic modeling study (Bountry et al., 2011) estimates the channel capacity in a 2-yr flow to be 100 $m^3 s^{-1}$, providing an upper limiting value for the bankfull capacity (Fig. 8).

Previous hydraulic models show that, in contrast to the mainstem, the unregulated lower South Fork has retained a capacity equivalent to the 1.5-yr to 3.5-yr recurrence interval flows, which is greater than the recurrence interval for the bankfull flow for most western Washington streams, which Castro and Jackson (2001) found averaged 1.2 yr. Modeling by KCM (1997) estimated an average bankfull capacity of 413 $m^3 s^{-1}$ (14,600 $ft^3 s^{-1}$), which exceeds the 2-yr flow (Table 3),

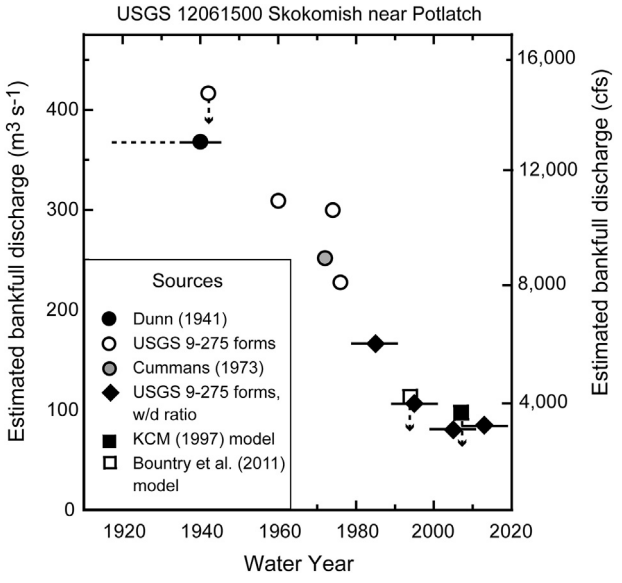

Fig. 8. Estimates of bankfull discharge in the Skokomish River at the USGS gauging station made from field estimates and hydraulic modeling, 1940–2007. Gauging station was located 1965–2016 at the Highway 101 bridge (Fig. 4B) and 1 rkm upstream in 1931–1964 (Fig. 4A). Types of estimates: (1) field observations published by the Army Corps of Engineers (Dunn, 1941) and USGS (Cummans, 1973); (2) field observations made by field personnel of the USGS and recorded in field measurement Form 9–275, (3) analysis of width-to-depth ratios for field measurements from Form 9–275, pooled by decade, (4) hydraulic modeling by KCM (1997) using 1994 channel topography data and by the Bureau of Reclamation (Bountry et al., 2011) using 2007 channel topography data. Horizontal bars indicate years of field measurements used for width-to-depth ratio estimate; vertical arrow indicates that estimate is a maximum estimate and actual value is lower than shown.

and modeling by Bountry et al. (2011) estimated the channel can contain about 80% of the 2-yr flow, which is equivalent to about the 1.5-yr flow (Table 3).

5.3. Historical change in channel planform in the Skokomish River valley

Much of the mainstem Skokomish River's historical channel capacity loss can be accounted for by channel narrowing; the 2015 channel was only 45% as wide as it was in 1938, the year of the earliest mainstem aerial photographs, having narrowed, on average, from 193 m in 1938 to 73 m in 2015 (Fig. 9A). Aerial photos show the channel narrowing as the establishment of closed-canopy riparian forest onto formerly unvegetated bars. About two-thirds of the post-1938 narrowing occurred between 1938 and 1951. While the 1938 photographs are the earliest of the mainstem, channel measurements made in 1924 for an engineering study (Jacobs and Ober, 1925) for the area between the North Fork confluence and the former Sunnyside Bridge at rkm 11.4 (Fig. 4A) agree closely to the area measured on the 1938 photographs (0.65 km^2 from the 1924 ground survey compared to 0.69 km^2 from the 1938 photos), suggesting the channel width changed little in the decade and a half prior to 1938.

In 1938, the channel was widest in the 2.4 rkm downstream of the North Fork confluence (Fig. 9B), and post-1938 narrowing was greatest in this same reach (Fig. 9C): the average channel width in 2015 was only 28% of the 1938 width (Fig. 9C). Downstream of this reach, the 2015 channel was 76% of the 1938 width (Fig. 9C).

Riparian canopy obscures the North Fork's channel downstream of the Cushman dams on aerial photos except for the lower 2.3 rkm where it flows on the Holocene alluvial fan built into the Skokomish Valley; in that reach, the active channel measured from aerial images in 2015 is 39% that of the area of the 1938 channel. A 2014 field-surveyed cross section and seven cross sections from lidar six river kilometers from the North Fork's mouth show that the channel averages 24% the width of that of the field-identified presumed pre-dam channel.

In contrast to the rapid narrowing of the mainstem and North Fork, the lower South Fork changed little overall, averaging 152 m in 1929 and 153 m in 2015 (Fig. 9A). The average width increased after 1938 to a maximum of 178 m in 1957 and then declined to 153 m in 1968.

5.4. Channel cross-sectional change in the Skokomish and lower South Fork Skokomish rivers

On average, bed elevation between Highway 101 and the South Fork gauge increased between 2007 and 2016 by 0.010 m yr^{-1}, and the sediment accumulation at cross sections averaged 1.79 $m^2 yr^{-1}$, totaling 20,400 $m^3 yr^{-1}$ (Fig. 10A and Table 4). In-channel sediment storage increased the most in the 1.3-km-long reach between the former (pre-2004) North Fork confluence and the Vance Creek confluence; storage also increased substantially in the 2.0-km-long reach between the former and current North Fork confluences (Fig. 4), the same reach that had narrowed most rapidly post-1940 (Fig. 9), and in the 1.7 km immediately upstream from Vance Creek (Fig. 10B). Farther upstream of Vance Creek, the South Fork degraded. Bed elevation changed the least downstream of the current (post-2004) North Fork confluence, which had a small net increase in bed elevation.

The overall rate of change in bed material storage in 1994–2007, 0.014 m yr^{-1}, is indistinguishable from that in the 2007–2016 period (the 1994–2007 comparison is less robust than the 2007–2017 comparison because elevations on the 1994 survey were more widely spaced than in the 2007 and 2016 surveys, and because the absence of horizontal control for the 1994 survey meant that relatively few cross sections could be compared in the most rapidly changing reaches). However, while the overall accumulation rate was unchanged between the two periods, the zone of greatest accumulation in 2007–2016 (shown by the dashed-line bar graph in Fig. 10A) shifted upstream compared to 1994–2007. In 1994–2007 there was more accumulation in the reach between Highway

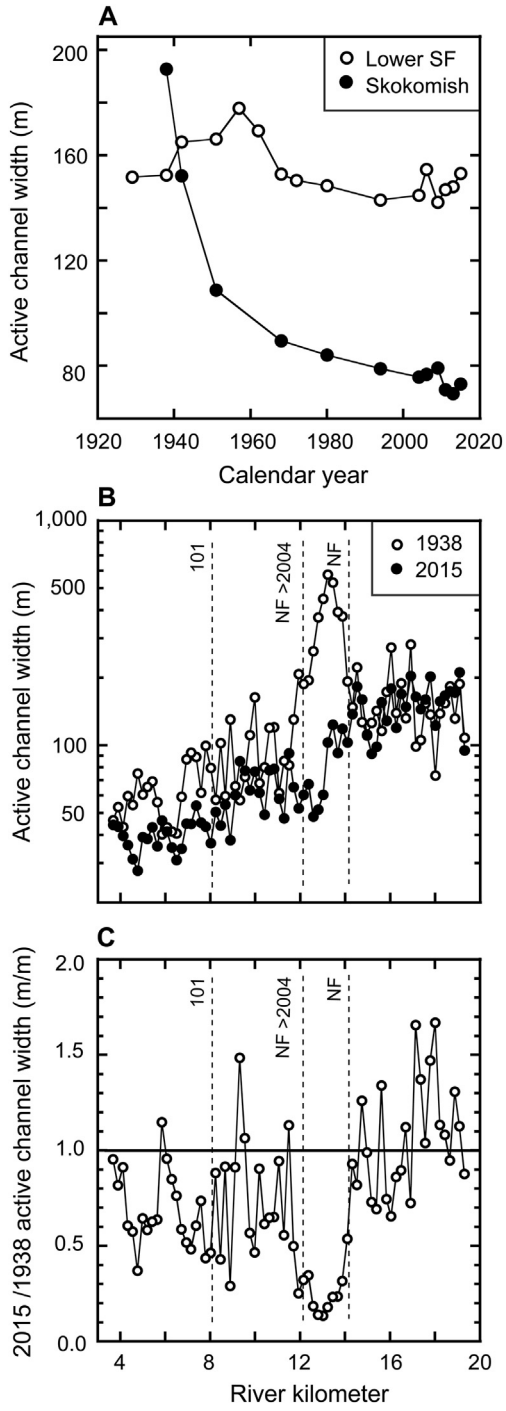

Fig. 9. (A) Change in channel width of the lower South Fork Skokomish River (hollow symbol) and Skokomish River (solid symbol) measured from aerial photographs, 1929–2015, from the South Fork gauge to Highway 101. Channel width is calculated from transects spaced at 200-m intervals along and perpendicular to a channel centerline generalized for the 1938–2015 period. (B) Active channel width in 1938 and 2015 at transects described above. (C) Active channel width in 2015 as a fraction of the 1938 active channel width for the same transects shown in Panel B; horizontal axis is the same as in panel B.

101 and the new North Fork confluence (0.007 m yr^{-1} in 2007–2016 compared to 0.019 m yr^{-1} in 1994–2007) and in the reach between the old and new North Fork confluences (0.032 m yr^{-1} in 2007–2016 compared to 0.040 m yr^{-1} in 1994–2007), and less in the upstream reaches, with the entire South Fork reach incising upstream of Vance Creek (Fig. 10A).

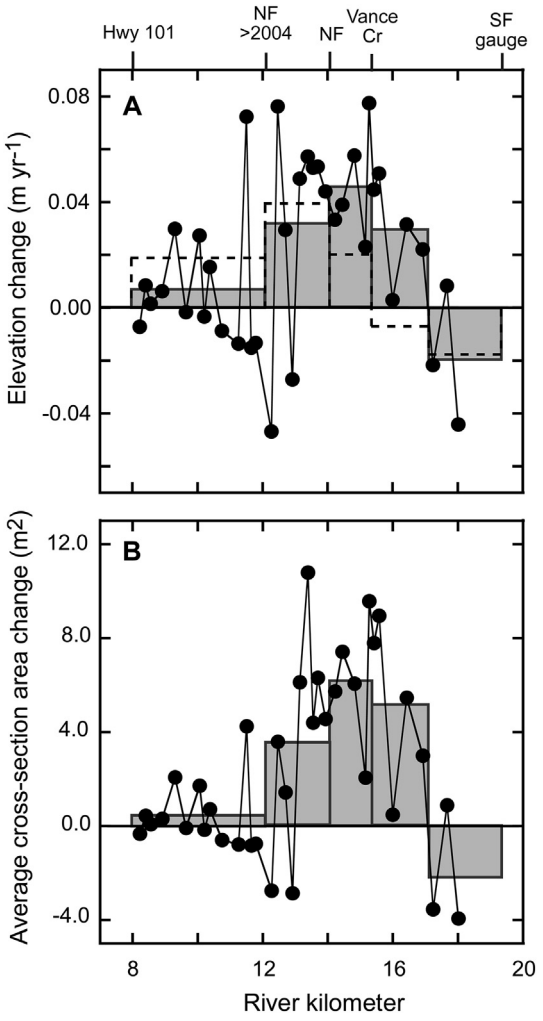

Fig. 10. Change in average bed elevation (A) and cross-sectional area (B), from comparison of cross sections surveyed in 2007 and 2016 on the Skokomish and lower South Fork Skokomish rivers. Bar graphs shows averages for river segments between the Highway 101 bridge and the current North Fork confluence, between the current and old North Fork, between the old North Fork and Vance Creek, and between Vance Creek and the South Fork USGS gauge. Dashed lines in panel (A) show the change in elevation from comparison of 1994 and 2007 cross sections.

5.5. Change in bed elevation recorded by stream gauges

The water surface elevation at the median annual flow at the mainstem gauge declined by about 0.3 m between 1932 and 1944 (Fig. 11A) after which the elevation remained roughly constant until 1966 (the gauge was moved downstream by 1 rkm in 1964; the two locations are shown in a single panel to facilitate visual interpretation). After 1966, the river's stage increased steadily at 0.041 m yr^{-1} in 1966–1998, after which the increase slowed moderately in each of the last two decades, to 0.034 m yr^{-1} in 1998–2007 and 0.029 m yr^{-1} in 2008–2016; this reduction in rate of elevation change at the gauge corresponds with the reduction in reach-averaged aggradation measured by cross sections in 2007–2016 relative to 1994–2007 between the new North Fork confluence and Highway 101 (Fig. 10). The overall increase in stage over the 50 yr between 1966 and 2016 is 1.84 m (Fig. 11A); the trend and amount of vertical change in the water surface are confirmed by change to the streambed elevation (Fig. 12). Additionally, Stover and Montgomery (2001) used field measurement notes from the gauge to show 1.3 m of positive bed elevation change through 1997, the same amount determined by our water-surface analysis for that period.

Table 4
Change in bed elevation (m yr^{-1}), average cross-sectional change (m^2 yr^{-1}), and volume (m^3 yr^{-1}), from comparison of cross sections measured in 2007 and 2016. Final column shows average change in bed elevation from comparison of cross sections measured in 1994 and 2007 (see text). Values for reaches are simple averages of values at cross sections within the reach. Totals for all reaches combined (final row in table) for volumetric estimates are sums of reach values, and for lowering and cross-sectional area change are averages of the reaches weighted by sub-reach length.

Reach	Reach length (river km)	2007–2016				1994–2007	
		Number of XS number (and avg. spacing, km)	Mean ± SE vertical change, m yr^{-1}	Mean ± SE cross-sectional change, m^2 yr^{-1}	Volumetric change ± SE, m^3 yr^{-1}	Number of XS (and avg. spacing, km)	Mean ± SE vertical change, m yr^{-1}
Mainstem: Hwy 101 to new NF confluence	4.1	14 (0.29)	0.007 ± 0.006	0.44 ± 0.38	1770 ± 1530	13 (0.31)	0.019 ± 0.005
Mainstem: New NF confluence to old NF confluence	2.0	9 (0.22)	0.032 ± 0.014	3.52 ± 1.46	6910 ± 2870	4 (0.49)	0.040 ± 0.005
SF: Old North Fork confluence to Vance Creek	1.3	5 (0.26)	0.046 ± 0.010	6.18 ± 1.23	8180 ± 1630	4 (0.33)	0.020 ± 0.008
SF: Above Vance Creek	1.7	5 (0.34)	0.030 ± 0.009	5.14 ± 1.55	8710 ± 2620	2 (0.85)	−0.006 ± 0.012
SF: Above Vance Creek to USGS gauge	2.4	3 (0.79)	−0.019 ± 0.005	−2.19 ± 1.55	−5200 ± 3670	4 (0.59)	−0.017 ± 0.040
Mainstem & SF weighted totals	11.4	36 (0.32)	0.010	1.79	20,400	27 (0.42)	0.014

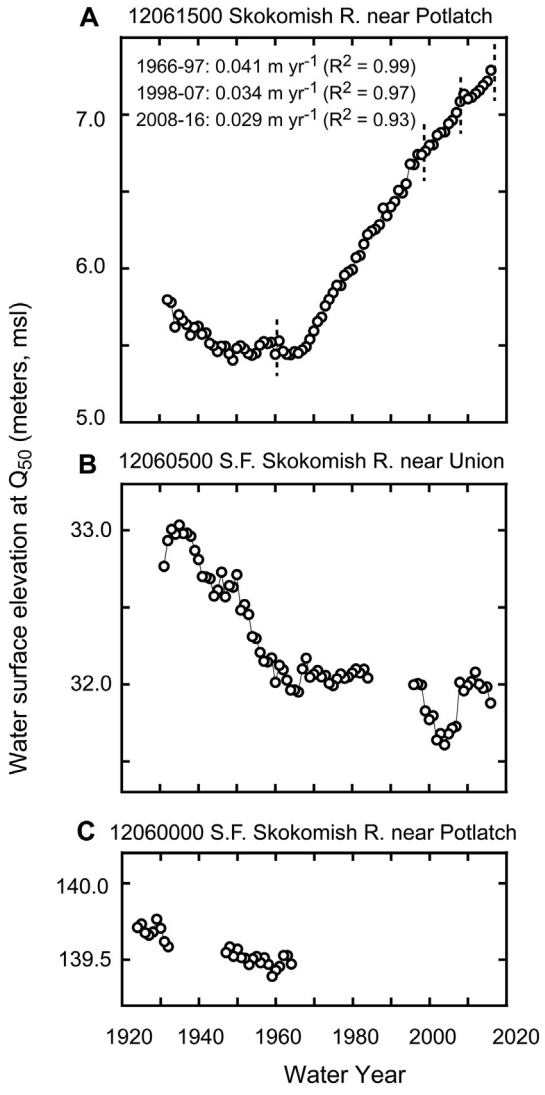

Fig. 11. Elevation of water surface at the 50% exceedance flow at three USGS gauges on the Skokomish and South Fork Skokomish rivers: Gaps in data indicate time periods when no field measurements were made. (A) Gauge 12061500, Skokomish River near Potlatch ("mainstem"). In 1964, the gauge was moved to its present location at Hwy 101 from its location 1.0 km upstream. (B) Gauge 12060500, South Fork Skokomish River near Union ("South Fork"); gauge was discontinued 1985–1994. (C) Gauge 1260000, South Fork Skokomish River near Potlatch ("upper South Fork"); gauge was discontinued 1933–1946 and after 1964.

At the South Fork gauge, the stage at the median flow gradually declined from 1930 to 1960 by about a meter; after a gap in the record in WY 1985–1994, the elevation declined further but had returned to the 1960 elevation by 2008 (Fig. 11B). At the gauge at the upper end of the South Fork's canyon (Fig. 1) there was an overall decline of about 0.2 m over a discontinuous record in WY 1923–1964 (Fig. 11C).

5.6. Sediment production in the upper South Fork

Channel widening accounts for the largest sediment source in the upper South Fork. The channel widened systematically over the course

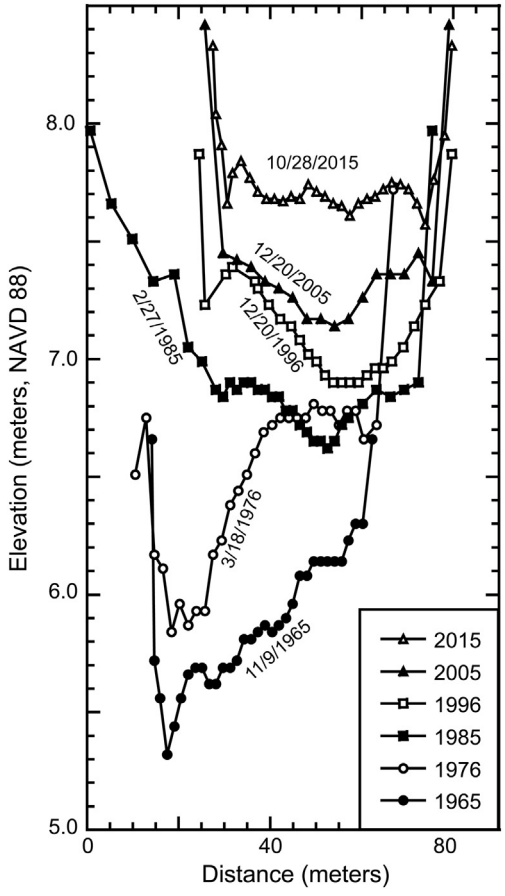

Fig. 12. Stream-bed elevation from gauging records at USGS gauge 12061500, Skokomish River near Potlatch, WA, 1965–2015. Representative cross sections are shown at approximately 10-yr intervals; discharge at selected cross sections ranged from 30.0 m^3 s^{-1} (1060 ft^3 s^{-1}) to 126 m^3 s^{-1} (4440 ft^3 s^{-1}).

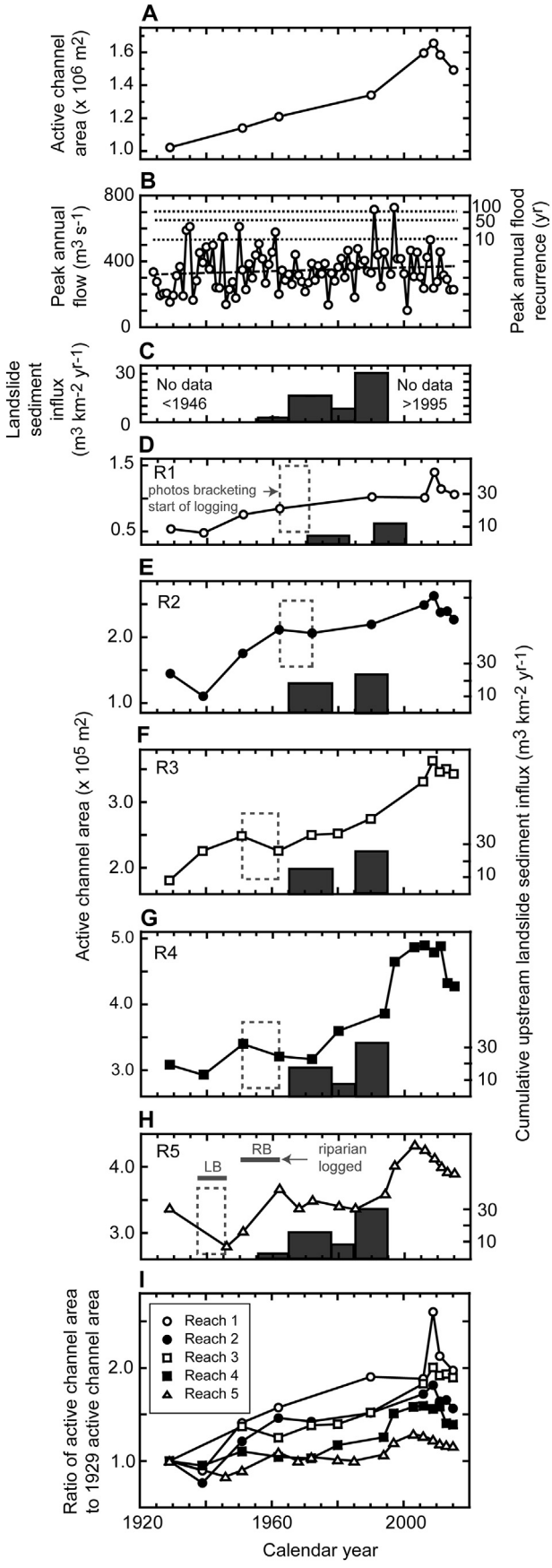

of the photo record, 1929–2015, with the 2015 channel area almost half again (146%) that of the 1929 channel area (Fig. 13A). This widening came at the expense of both glacial terraces and floodplains. Field-measured heights of terrace bluffs ranged from 6 m to 55 m and averaged 22 m; applying bluff heights to areas eroded from 1990/1994 to 2015 indicates an erosion of 112,000 $m^3\ yr^{-1}$ or 220,000 Mg yr^{-1}, or 1100 Mg $km^{-2}\ yr^{-1}$ averaged over the South Fork exclusive of the Vance Creek drainage. Bank erosion of forested floodplain resulted in an additional 18,000 $m^3\ yr^{-1}$ (30,000 Mg yr^{-1}) of sediment.

By comparison, landsliding has been a much smaller sediment source. According to a 1946–1995 landslide inventory (WADNR, 1997a), sediment from landslides in the South Fork (including Vance Creek; Fig. 1) delivered to streams an estimated 7500 Mg yr^{-1} or 28 Mg $km^{-2}\ yr^{-1}$; 90% of inventoried landslides, by number, were related to logging, and most failures were associated with roads. The landsliding rate varied throughout the inventory period; almost half (48%) of landslide-derived sediment by volume delivered to streams was in 1985–1995 and another 27% in 1965–1978. Landslide inventories made from aerial photographs generally do not detect all landslides and consequently underestimate sediment production; for example, Brardinoni et al. (2003) found, in the 198-km^2 Capilano River basin in western British Columbia, that landslides not detectable from aerial imagery alone accounted for an additional 30% by volume. Applying this figure to the sediment delivery estimated by the South Fork inventory would increase sediment deliver to 38 Mg $km^2\ yr^{-1}$. The inventory also included landslides that did not deliver sediment to channels; including these landslides indicate overall erosion rates of 34 Mg $km^2\ yr^{-1}$ or 44 Mg $km^2\ yr^{-1}$ including the adjustment for undetected landslides. This landslide erosion rate is low relative to the regional average, but within the range of variability determined by Smith and Wegmann (2018) by mapping landslides for the 1990–2015 period in a 15-km by 85-km, SW-NE-trending swath across the Olympic Mountains.

5.7. Sediment flux to the Skokomish Valley

The suspended sediment flux calculated at the Highway 101 gauge, for the WY 1944–2017 period is 242,000 Mg yr^{-1}, or 712 Mg $km^{-2}\ yr^{-1}$ averaged over the 340 km^2 area that excludes the 248 km^2 area upstream of Cushman Dam No. 2 (Table 5). Combining this with the estimated bedload of 70,500 Mg yr^{-1} or 207 Mg $km^{-2}\ yr^{-1}$ indicates a total load of 919 Mg $km^{-2}\ yr^{-1}$. The net change in bed material storage in the lower South Fork and the Skokomish River upstream of Highway 101, from Table 4, is 34,000 Mg yr^{-1}, or 101 Mg $km^{-2}\ yr^{-1}$ if averaged over the basin exclusive of the area draining to Lake Cushman; adding this to the estimated total flux at Highway 101 (919 Mg $km^{-2}\ yr^{-1}$) to estimate the total influx of sediment to the Skokomish River mainstem yields 347,000 Mg yr^{-1} or 1020 Mg $km^{-2}\ yr^{-1}$ (Table 5).

6. Discussion

We use the geomorphologic evidence, described above, to evaluate three hypotheses that have been advanced to explain the channel capacity loss and increased flooding in the Skokomish River mainstem, as summarized in Table 6, and to evaluate several possible controls on high sediment yields from lateral channel erosion in the South Fork basin.

Fig. 13. Change through time in active channel area, 1929–2015, peak annual flows, and landslide sediment input to the upper South Fork Skokomish River. (A) Active channel area for all photo years for which complete coverage of the study area was available. (B) Peak annual flood for the South Fork near Union gauge, USGS 12060500, from Fig. 7. Horizontal dotted lines show magnitude of 10-yr, 50-yr, and 100-yr recurrence floods, from Table 3. Dashed line shows weak, insignificant trend line. (C) Volumetric sediment influx to channels in the study reach for five periods from 1946 to 1995, from WADNR (1997a). (D)–(H) Change through time in active channel area for five reaches (Fig. 6A), 1929–2015, arranged from upstream to downstream. Also shown (bars) is cumulative sediment influx from landsliding to the reach and from upstream. (I) Percentage increase in active channel area relative to 1929 active channel area for the five reaches, 1929–2015.

6.1. Evaluation of the Cushman flow reduction hypothesis

6.1.1. Channel capacity loss

In regulated rivers such as the Skokomish, where flow regulation substantially reduces the frequency of sediment-transporting flows and there is a high ratio of sediment supply downstream of a dam relative to the supply upstream of the dam, channels are expected to aggrade and narrow (e.g., Brandt, 2000; Grant et al., 2003). Capacity loss in the Skokomish River, in its onset and persistence (Fig. 8) and its spatial pattern (Figs. 9 and 10), is consistent with the expected channel response. Capacity loss began in the decade following the out-of-basin export of water that began with the completion of Cushman No. 2 in 1930. The rate of capacity loss has also been relatively constant, consistent with a ramped disturbance such as flow reduction rather than a pulsed disturbance such as an upstream sediment pulse. In addition, there has been no capacity loss in the lower South Fork (see Section 5.2) except presumably in the first 3 rkm upstream of the North Fork confluence.

6.1.2. Channel narrowing

The timing, rate of change, magnitude, and spatial extent of channel narrowing in the mainstem Skokomish River are consistent with the expected response to flow reduction. Narrowing was most rapid in the first few decades following flow regulation (Fig. 9), consistent with published case studies of the channel response to flow regulation in which most channel width adjustment occurs within the first few decades following dam closure. For example, a study of downstream change to 21 dams on alluvial rivers found that 95% of channel width adjustment occurred within a modal value of 35 yr (Williams and Wolman, 1984). That the mainstem Skokomish River's channel width measured in 1924 by Jacobs and Ober (1925) is close to that measured from the 1938 aerial photos suggests a response time of about a decade before the channel began to narrow, which is consistent with the time needed for riparian trees to colonize and narrow the channel. Further support for mainstem channel narrowing being a response to flow reduction is provided by the narrowing of the North Fork's channel downstream of the Cushman dams. In addition, well-established theory in geomorphology predicts that channel width will adjust to the magnitude of channel-forming flows (e.g., Knighton, 1998).

That the width of the lower South Fork did not change systematically while that of the mainstem did (Fig. 9A) is also consistent with the flow reduction hypothesis. Narrowing of the mainstem without narrowing in the lower South Fork cannot be explained as an adjustment to a hypothetical, exceptionally large flood in the North Fork in the decade or two prior to the 1938 photos because floods from the North Fork in this period would have been modulated by the Cushman Reservoir since closure of Cushman No. 1 in October 1925 (Perrin et al., 2014) and essentially eliminated by diversion of water out of the basin upon the completion of Cushman No. 2 in 1930 (USDOE, 2010); additionally, the channel width remained essentially unchanged, or increased slightly, between that measured in 1924 by Jacobs and Ober (1925) to the 1938 aerial photos. Moreover, the persistence and amount of narrowing likely far exceeds the response to a hypothetical large flood.

6.1.3. Channel bed-elevation change

Change to the channel bed elevation observed at cross sections since 1994 is consistent with the expected response to flow reduction. Aggradation measured in both 1994–2007 and 2007–2016 was greatest near the North Fork confluence but in both periods extended downstream throughout the surveyed reach of the mainstem and decreased rapidly upstream of the North Fork's confluence, transitioning to degradation in the South Fork (Fig. 10, Table 4). That the zone of greatest accumulation progressed upstream from the 1994–2007 period to the 2007–2016 period could be a consequence of the rapid channel filling in the two river kilometers downstream of the old North Fork, which would diminish the upstream channel gradient and promote an upstream-progressing depositional wedge.

The three-decade-long lag between completion of the Cushman Project and the onset of aggradation at the Highway 101 gauge complicates flow reduction as an explanation for the post-1966 increase in bed elevation at the gauge. This lag time led previous investigators to speculate that other factors such as flow constriction by levees or upstream sediment supply might partially (Stover and Montgomery, 2001; Bountry et al., 2009) or entirely (Simons and Simons, 1997; Curran, 2016) explain the trend. However, there are both local and systemic controls that could plausibly account for the three-decade response time. USGS field technicians observed that dredging for gravel supply in the first half of the 1930s influenced the hydraulic control and caused the river to shift. This is consistent with the timing of channel bed (Fig. 5 in Stover and Montgomery, 2001) and water surface (Fig. 11A) lowering at the mainstem gauge. Later in the 1930s, two channel meanders 1.7 rkm downstream of the gauge were cut off (Fig. 4), which could also have caused incision to progress upstream to the gauge. The gradual decline in bed elevation before about 1950 mirrors a decline in that period at the South Fork gauge (Fig. 11B), 10 rkm upstream, and could also reflect trends in sediment supply.

A potential systemic explanation for the three-decade response time at the gauge is a complex channel response (Schumm, 1973) to flow reduction. Immediately following flow reduction, before the channel began to narrow, the wide mainstem channel in the few kilometers immediately downstream of the confluence (Figs. 4A and 9) would have had a limited sediment transport capacity. The channel narrowed over the following decades, especially in the few kilometers immediately downstream of the North Fork confluence, as sediment accumulated in bars, which were subsequently colonized by pioneering riparian tree species. This channel narrowing and associated increased bankfull flow depth would have partially compensated for the channel shallowing and flow reduction, thereby increasing the channel's capacity to transport sediment downstream to the USGS Highway 101 gauge. This explanation is consistent with the evidence and physically plausible, but speculative. There are few documented cases of systemic aggradation downstream of dams, and the timescale and nature of such a response is not well understood.

The mid-1960s onset of aggradation at the gauge could also reflect an increase to the river's sediment load associated with the lateral fluvial erosion of terraces and floodplains in the upper South Fork. The widening rate has been roughly constant overall since the earliest aerial

Table 5
Sediment flux at the mainstem Skokomish River gauge at Highway 101, determined from suspended and bedload sediment measurements made by the USGS and by Simons and Associates, as described in the text, for the period of record (WY 1944-WY 2017); change in channel sediment storage, measured by repeated cross sections, 1994–2016, in the lower SF and mainstem (from Table 4), and sediment supply to the Skokomish Valley, determined by summing the export at the mainstem gauge and the estimated change in channel storage. Specific sediment yields are determined by dividing sediment yield by the 340 km^2 upstream of the mainstem gauge exclusive of the area upstream of the Cushman Projects that do not contribute sediment to the mainstem.

Sediment flux at Highway 101 mainstem USGS gauge						Change in channel storage, lower SF and mainstem		Inferred sediment supply to the Skokomish Valley	
Suspended sediment load		Bedload		Total load					
Mg yr^{-1}	Mg km^{-2} yr^{-1}	Mg yr^{-1}	Mg km^{-2} yr^{-1}	Mg yr^{-1}	Mg km^{-2} yr^{-1}	Mg yr^{-1}	Mg km^{-2} yr^{-1}	Mg yr^{-1}	Mg km^{-2} yr^{-1}
242,000	712	70,500	207	313,000	919	34,000	101	347,000	1020

Table 6
Summary of evidence for and against three hypotheses on the cause of aggradation in the Skokomish River.

Hypothesis	Supports or contradicts hypothesis	Evidence
Flow regulation by Cushman Project	Supports	• Bankfull channel capacity loss from combined changes to width and bed elevation: (a) began about a decade after flow regulation, (b) has been roughly constant in subsequent eight decades, (c) occurred in mainstem but not lower South Fork. • Channel narrowing: (a) began about a decade following flow regulation and was most rapid in the subsequent few decades, consistent with timing of channel adjustment observed downstream of dams elsewhere, (b) occurred in North Fork and mainstem but not lower South Fork, (c) is consistent with well-established theory in geomorphology as a response to reduced channel-forming discharge. • Channel aggradation: Mainstem has aggraded, but lower South Fork, aside from immediately upstream of the North Fork confluence, has not.
	Equivocal support	• Aggradation at mainstem gauge began several decades after flow regulation began, but this delay can be explained by some combination of gravel mining and channel straightening near the gauge, a complex response to flow regulation, or possibly by natural increase to the sediment supply from the upper South Fork beginning in the early twentieth century.
Levees along mainstem	Contradicts	• Levees were built several decades after most narrowing occurred and after aggradation had begun at the mainstem gauge. • Levee location is inconsistent with causing aggradation: (a) levees are discontinuous, (b) where present, levees are generally on one side of the river, (c) levees are set back from river and do not confine it, and (d) while entire mainstem narrowed and shallowed, there are no levees along about two-fifths of the mainstem, including near the mainstem gauge, where nearly 2 m of aggradation has been recorded.
Pulse of increased sediment supply from logging in the upper South Fork	Contradicts	• Mainstem channel capacity loss: (a) began before substantial upstream logging, and (b) relatively steady rate of change over eight decades is inconsistent with transient change to sediment supply as cause. • Channels are generally observed to widen in response to upstream sediment pulse, but lower South Fork did not widen and mainstem narrowed. • No evidence for passage of aggradational bed wave in the logging era at either of the South Fork gauges. • Greatest rate of mainstem sediment accumulation appears to have shifted upstream from 1994–2007 to 2007–2016, opposite to expected downstream progression of bed wave. • Amount of sediment from logging-related landslides is much less than volume of sediment from upper South Fork channel widening and much less than mainstem channel capacity loss. • The upper South Fork's riparian forest largely remains old-growth forest, ruling out riparian logging as cause of channel widening of the upper South Fork.
	Equivocal support	• Logging-associated landslides could have indirectly promoted channel widening in upper South Fork but cannot be a primary cause because much of the widening predates logging and associated landslides.

photo measurement in 1929 (Fig. 13A), but it is unknown when the widening trend began. Assuming the trend began within a few decades of the twentieth century, published observations of downstream-translating sediment waves (e.g., Beschta, 1983; Griffiths, 1993; Madej and Ozaki, 1996, 2009; Nelson and Dube, 2015) suggest that this initial increase in sediment load could possibly have arrived in the mainstem by the 1960s. An early-twentieth century increase in sediment load could also explain the transient widening in the lower South Fork in the 1940s and 1950s (Fig. 9A). However, if this is the case, it's not clear why the lower South Fork's planform response, as well as the bed elevation response at the South Fork gauge, were transient while the sediment supply from channel widening has remained roughly constant (Fig. 13A) or why the mainstem gauge response (Fig. 11A) has persisted for more than five decades. Nevertheless, it remains possible that an early-twentieth century increase to the sediment load from the South Fork could at least partially explain why aggradation recorded at the mainstem gauge began in the 1960s.

6.2. Evaluation of levee construction hypothesis

Neither the timing nor location of levee building is consistent with the observed channel response. As indicated previously, while 1 rkm of levee was built in 1968, the other 4 rkm of levees were not built until the 1980s and 1990s, after most channel narrowing had already occurred, and several decades after aggradation began at the Highway 101 gauge in the mid-1960s (Fig. 4B). Moreover, where levees have been built they are discontinuous, generally on one side of the river, and set back from the river by 0.1–0.2 km and do not constrict the river (Fig. 4B). There are no levees in the lower two-fifths of the mainstem between the historic North Fork confluence and the mainstem gauge, but the entire reach narrowed and aggraded, and the mainstem gauge, which has recorded nearly 2 m of aggradation, is two river kilometers downstream of the leveed reach. Finally, even if levees had been constructed continuously along the river and had confined it artificially, it's unclear whether a gravel-bed river channel would respond by aggrading or if confinement would promote greater transport capacity and resulting incision (e.g., Gendaszek et al., 2012; Leonard et al., 2017).

6.3. Evaluation of logging-induced sediment-wave hypothesis

The hypothesis that logging-related landsliding triggered a downstream-moving wave of sediment can be tested against expectations from case studies of channels adjusting to increased rates of coarse sediment supply. Relevant case studies include: sediment sourced from mining debris (e.g., Gilbert, 1917; Knighton, 1989; James, 1991; Bertrand and Liebault, 2018), which provides a reasonable analog to a sustained period of elevated logging-induced sediment influx because coarse sediment supply from mining operations tends to remain elevated for decades; sediment eroded from reservoirs following dam removals (e.g., East et al., 2015; Major et al., 2017); and sediment sourced from hillslopes following logging, although sediment influx in the available, well-documented cases is dominated by the effects of a single, unusually-large storm event (e.g., Beschta, 1983; Madej and Ozaki, 2009; Nelson and Dube, 2015). Based on these case studies, the expectation is that a sediment wave, or bed wave (James, 2006), would cause channel widening and aggradation and that as the bed wave works its way downstream, the channel incises and narrows, beginning upstream and progressing downstream. In addition to the expected plan-form record of change, a bed wave's passage should also be recorded by transient bed elevation change at cross sections or stream gauges (e.g., Gilbert, 1917; James, 1991; Jacobson and Gran, 1999; Madej and Ozaki, 2009; East et al., 2015).

Overall channel capacity loss (Fig. 8) cannot be explained by logging in the upper South Fork because capacity loss began prior to substantial steep-land logging (Fig. 6) or logging-associated landslides (Fig. 13) in

the upper South Fork. Additionally, the rate of capacity loss has been relatively constant for nearly eight decades (Fig. 8), contrary to the expected temporal pattern to change resulting from a transient sediment wave.

The historical change to channel width, in both its temporal and spatial patterns, contrasts with the expected response from a sediment bed wave from logging-associated landslides. While the upper South Fork widened through time, the widening began prior to logging and so the channel widening cannot be explained primarily as a response to sediment influx from landslides (see Section 6.4). The lower South Fork channel width did not change overall from 1929 to 2015, but there was a transient widening in the 1940s and 1950s (Fig. 9A), consistent with the possible response to an increase to sediment supply. However, the period of logging-related landsliding in the upper South Fork (Fig. 13) did not begin until the decades after the lower South Fork's transient widening (Fig. 9A), whereas the presumed early-twentieth century increase to supply from bank and bluff erosion in the upper South Fork precedes the lower South Fork's response. Most problematic for the logging hypothesis is that in the decades since logging-related landsliding began (Fig. 11), the mainstem has narrowed (Fig. 9A), opposite to the widening expected from an increased sediment load.

Neither is the observed channel-bed elevation response consistent with expectations of the logging-induced sediment bed wave hypothesis. The passage of a sediment wave should be evident in the South Fork's stream gauging records (Fig. 11B and C) in the decades preceding aggradation at the mainstem gauge. However, the streambed at the South Fork gauge, 10 rkm upstream, declined gradually by about 1 m between 1935 and 1960 (Fig. 11B). Discontinuous records from the upper South Fork gauge (Fig. 11C), 10 rkm upstream from the mainstem gauge, at the upper entrance to the South Fork's gorge (Fig. 1, Table 1), also show an overall decline from 1923 through 1964, consistent with the passage of a bed wave through the upper end of the South Fork gorge before the early 1920s (Fig. 11C) and the lower end of the gorge by about 1930 (Fig. 11B). Because there had been essentially no upstream land management before 1929, any such sediment wave would have been unrelated to land use. The 1923–1964 decline in bed elevation at the South Fork gauge is consistent with the possibility of incision in the wake of a sediment wave prior to the 1920s, but this would have been decades before any logging in the South Fork watershed. Additionally, the two-decade cross-sectional record of bed elevation change shows the opposite of a downstream-progressing sediment wave, as the zone of maximum accumulation appears to have shifted upstream between the 1994–2007 and 2007–2016 periods rather than translating downstream (Fig. 10A).

Finally, the volume of logging-generated sediment is too small to explain the observed downstream aggradation. The relatively constant supply of sediment from lateral channel erosion of glacial terraces and the floodplain (254,000 Mg yr^{-1} from the upper South Fork valley alone) is much larger than the sediment supplied by landsliding (9800 Mg yr^{-1} from the South Fork and Vance Creek watersheds combined).

6.4. Potential controls on, and quantitative significance of, sediment yields from the South Fork basin

Lateral channel erosion in the upper South Fork has resulted in sediment yields that are high (Table 5) and, based on the rate of lateral channel erosion, have presumably been high for at least the nine decades of the aerial photo record. As discussed in Sections 6.1 and 6.3, a presumed increase to the sediment yield in the early 20th century could possibly explain some of the types of evidence for downstream channel response. However, high sediment yields cannot have been the primary cause of downstream channel capacity loss in the mainstem Skokomish River: only flow regulation can explain the record of channel narrowing, and while the record of channel aggradation is less temporally and spatially continuous than the plan-form record and is thus ambiguous and open to multiple potential interpretations, flow regulation best accounts for the evidence for channel aggradation. However, because high sediment yields likely influence the magnitude of downstream capacity loss, understanding the cause of high rates of lateral channel erosion in the upper South Fork is important for understanding mainstem channel capacity loss.

We evaluate three potential causes of the progressive widening and resulting lateral fluvial erosion of terraces and floodplains in the upper South Fork: riparian logging and subsequent loss of bank strength; increases through time in peak flows; and influx of sediment from landsliding. Riparian logging along the South Fork can be ruled out as a cause because, almost along its entire length, the upper South Fork's riparian forest remains old growth except for parts of the downstream-most segment (Fig. 6). The streamside forest in that segment was logged in 1939–1946 on the left bank and in 1951–1962 on the right bank side in preparation for a planned hydroelectric project (Bair and McHenry, 2011), and the channel widened during these periods (Fig. 13H), but the widening is not more rapid than in some other segments where the riparian forest remained unlogged.

Peak annual flows have not increased systematically during the period of record. The size and concentrations of individual peak flows do correlate with fluctuations in the rate of channel expansion; the 1934–1961 and 1991–1997 periods, which have a concentration of peak flows exceeding the 10-yr recurrence (Fig. 13B), correspond to more rapid rates of increase in channel width, particularly the later period, which contained the flood of record (Fig. 13A). This second period of accelerated widening persisted until 2009, 11 yr after the 1997 flood, after which the channel narrowed. Field and aerial photo observations indicate this narrowing occurs as point bars and mid-channel islands are colonized by red alder (*Alnus rubra*), black cottonwood (*Populus trichocarpa*), and willow (*Salix spp.*) and as the channel incises; September 2013 and 2014 field observations show that the channel had begun to incise in at least the upper and middle part of the valley, creating incipient terraces of colonizing forest. As of 2015, post-1997 flood channel narrowing had resulted in a channel area consistent with the general linear increase throughout the 1929–2015 period (Fig. 13A). However, these fluctuations do not explain the systematic, long-term widening.

Finally, neither the timing nor location of sediment influx from mass wasting (Fig. 13C) is consistent with being the primary cause of channel widening. Forest-practice related landsliding began decades after the onset of widening (Fig. 13A) and there was substantial widening in the upper reaches (Fig. 13D-E) prior to any logging or road building in or upstream of those reaches. Additionally, the increase in channel area as a percentage increase is greatest in the upstream-most segments and least in the downstream-most segments (Fig. 13I), whereas the specific sediment influx from landslides increases in a downstream direction (Fig. 13D-H), also arguing against the role of logging-derived landslides as a cause of downstream widening.

The quantitative significance of individual sediment sources from the South Fork is demonstrated by comparison to the estimated total supply of sediment to the Skokomish Valley, taken as the sum of the flux of suspended and bedload sediment in the Skokomish River at the Highway 101 bridge and the change in bed material stored in the mainstem and lower South Fork, or 347,000 Mg yr^{-1} or 1020 Mg km^{-2} yr^{-1} (Table 5). Sediment production from widening of the upper South Fork alone (i.e., exclusive of terrace or floodplain erosion by Vance Creek or the North Fork downstream of the Cushman Projects) accounts for 254,000 Mg yr^{-1} (224,000 Mg yr^{-1} from bluff erosion and an additional 30,600 Mg yr^{-1} from floodplains), or about three-fourths (73%) of the total 347,000 Mg yr^{-1} of sediment estimated to be contributed to the Skokomish River valley.

The South Fork's sediment yield is similar to yields from two basins in western Washington also having extensive paraglacial sediment sources; the Stillaguamish River transported 840 Mg km^{-2} yr^{-1} in suspended load alone (Anderson et al., 2017) and the South Fork Nooksack River transported 808 Mg km^{-2} yr^{-1}, also in suspended sediment alone

(Anderson et al., unpublished data). In contrast, suspended sediment loads from three basins immediately adjacent to the Skokomish and not having a significant paraglacial sediment source, the Hamma Hamma, Duckabush, and Dosewallips rivers, range between 48 and 87 Mg km^{-2} yr^{-1} (Czuba et al., 2011).

6.5. Implications

This study demonstrates that an examination of geomorphic evidence from existing records and aerial photographs, supplemented with limited field measurement, can distinguish among multiple potential causes of channel capacity loss and associated flooding. The morphological evidence for channel change associated with the historical, progressive loss of channel capacity in the mainstem Skokomish River is consistent in its nature, spatial distribution, timing, and rate of change, with flow reduction from the Cushman Projects in combination with a naturally high sediment supply to the river's South Fork, whereas most of the evidence is inconsistent with the logging-related landslides and levee hypotheses (Table 6).

The morphological evidence suggests the possibility that the Skokomish River's response to flow reduction was complex, temporally and spatially: The channel rapidly narrowed in the first few decades following flow regulation, especially proximal to the dam. Channel bed aggradation, at least at the downstream gauge, was not apparent for a few decades, possibly reflecting a delay in downstream sediment transport while the channel narrowed and maintained transport capacity. In addition, cross-sectional comparisons suggest that aggradation in the last decade, nine decades following dam completion, is progressing upstream and extending above the North Fork confluence.

While hydroelectric dams generally tend to reduce downstream flooding, the Cushman Project, despite greatly reducing downstream flows, has, instead, worsened downstream flooding by reducing channel capacity by narrowing and shallowing the channel. This paradoxical effect resulted from the unusual combination of the Cushman Project's operations, which exports most of the North Fork's flow out of the basin, the existence of a natural lake at the dam site that limited pre-Project sediment production from the North Fork, and the watershed's geologic history, which promotes high sediment yields from the South Fork and makes the mainstem Skokomish River a natural depositional reach. While flow regulation typically stabilizes downstream channels, in this case flow regulation and consequent loss of channel capacity has increased the likelihood of a large-scale channel avulsion to the south side of the floodplain (Sofield et al., 2007).

This case study highlights the importance of evaluating potential geomorphic and flooding effects of existing and planned dams, and dam removals, in light of a dam's operation and the watershed's geology and physiography. In particular, it underscores the potential importance of tributaries downstream of dams (for review, see Grant, 2012), or, more broadly, downstream sediment sources; in this example, the tributary effect is exaggerated by the large flow reduction in the North Fork and the high rates of sediment production from the downstream South Fork tributary. A recent survey of 52 stream gauges in Washington State (Pfeiffer et al., 2018) found that streambeds are generally stable except downstream of glaciers. One of the few instances in the survey of rapid bed aggradation at a gauge not downstream of a glacier is downstream of a dam in the Cedar River (Gendaszek et al., 2012); there, similar to the upper South Fork Skokomish, lateral stream erosion of glacial bluffs downstream of the dam are a dominant sediment source (Perkins Geosciences, 2002).

We could not determine a cause for the channel widening and glacial terrace erosion responsible for high sediment yields from the South Fork, but the hydrologic change literature suggests a possible, speculative explanation. Hydrologic models show that in the Puget Sound region, and the Skokomish watershed in particular, the runoff regime has shifted since the late nineteenth century from snow-melt dominated toward rain dominated (Cuo et al., 2009), and that this trend, which is expected to continue, includes higher peak flows (Lee et al., 2015). This raises the possibility that the post-1929 channel widening, and associated lateral erosion of glacial terraces, is a long-term response to shifts in the dominant runoff regime that began before the installation of stream gauges in the 1920s. Such a shift toward higher, rain-dominated runoff peaks could be initiating a renewed cycle of paraglacial sedimentation driven by climate change; if this is the case, it could have implications for sediment yields regionally.

An understanding of the root causes of functional losses to rivers and their habitats is necessary for designing restoration measures that can reasonably be expected to remedy lost function (e.g., Beechie et al., 2010). In the Skokomish River, large scale restoration has been underway, despite a lack of clarity about the causes of aggradation and associated habitat and flooding problems in the river (e.g., USACOE, 2014). An emphasis on road rehabilitation, sediment source reduction, and building in-channel structures in the upper South Fork, while important for reducing sediment production and improving local habitats, cannot be expected to remedy channel capacity loss and flooding downstream in the Skokomish Valley. Similarly, an emphasis on levee removal or setback (USACOE, 2014) while enhancing channel and floodplain habitats, does not address the underlying causes of channel capacity loss, which is the narrowing and shallowing of the channel due to flow reduction. This study illustrates the value to restoration planning of undertaking a systematic analysis of the multiple, potential causes of functional loss, in this case the progressive loss to the Skokomish River's channel capacity.

7. Conclusions

The Skokomish River's channel capacity has been reduced more than three-fold over the last eight decades. Analysis of aerial photographs, repeated cross-section surveys, and USGS gauging records show this capacity loss was due to both a narrowing and shallowing of the channel associated with flow regulation. Channel narrowing, which is consistent with the expected response to flow regulation, began within about a decade of the start of water export from the basin, and was initially rapid, consistent with observations downstream of other dams. Channel filling at a downstream gauge was delayed by up to three decades, possibly as a complex response of downstream narrowing followed by shallowing, but also possibly as a result of a natural increase to the sediment supply of the river's South Fork that presumably began sometime before 1929. While two competing explanations have been proposed as explanations for the historical channel capacity loss, neither mainstem levee construction or logging-related erosion in the South Fork basin are consistent with the nature or timing of channel response. While hydroelectric dams typically reduce flood peaks, in the Skokomish River basin the unusual combination of dam operations and the basin's controls on sediment production create the paradoxical effect of worsening flooding by reducing channel capacity; this highlights the importance of assessing downstream effects of dams in context of dam operations and basin geology and physiography.

Acknowledgments

This study grew out of a case study for a course in applied fluvial geomorphology taught at the University of Washington by the senior author in which the co-authors were students. We thank Jennifer Bountry, U.S. Bureau of Reclamation and Karl Eriksen, U.S. Army Corps of Engineers, for providing cross sectional data, Andy Gendaszek, USGS Water Resources Division, for his assistance with accessing archived gauging records, and Amber Mount and Eric Beach at Green Diamond Resources Company for providing access to aerial photography and for access to Green Diamond properties in the North Fork Skokomish watershed. We also thank Jon Beyeler, Sean Connor, Jenny Hu, Matthew Porter, and Tina Andry for field assistance, and Kurt Hunter for logistical support, for the 2016 channel cross section survey. The manuscript benefited greatly from comments by Derek Booth on an earlier draft and the comments of two anonymous reviewers.

References

Anderson, S.W., Curran, C.A., Grossman, E.E., 2017. Suspended-sediment loads in the lower Stillaguamish River, Snohomish County, Washington, 2014–15. U.S. Geological Survey Open-File Report 2017–1066 https://doi.org/10.3133/ofr20171066 (10 p).

Arcos, M.E.M., 2012. A Holocene sedimentary record of tectonically influenced reduced channel mobility, Skokomish River delta, Washington State, USA. Geomorphology 177-178, 93–107. https://doi.org/10.1016/j.geomorph.2012.07.016.

Bair, B., McHenry, M., 2011. South Fork Skokomish stream corridor rehabilitation. Abstract 78-23 presented at 2011 American Fisheries Society 141st Annual Meeting, Seattle, Washington, September 4-8, 2011.

Beale, H., 1990. Relative Rise in Sea-Level during the Past 5000 Years at Six Salt Marshes in Northern Puget Sound, Washington. Shorelines and Coastal Zone Management Program. Washington Department of Ecology, Olympia, WA.

Beechie, T.J., Sear, D.A., Olden, J.D., Pess, G.R., Buffington, J.M., Moir, H., Roni, P., Pollock, M.M., 2010. Process-based principles for restoring river ecosystems. Bioscience 60, 209–222. https://doi.org/10.1525/bio.2010.60.3.7.

Bertrand, M., Liebault, F., 2018. Active channel width as a proxy of sediment supply from mining sites in New Caledonia. Earth Surf. Process. Landf. https://doi.org/10.1002/esp.4478.

Beschta, R.L., 1983. Long-term changes in channel-widths of the Kowai River, Torlesse Range, New Zealand. N. Z. Hydrol. Soc. 22, 112–122.

Booth, D.B., 1994. Glaciofluvial infilling and scour of the Puget Lowland, Washington, during ice-sheet glaciation. Geology 22, 695–698. https://doi.org/10.1130/0091-7613(1994)022<0695:GIASOT>2.3.CO;2.

Bountry, J.A., Godaire, J.E., Klinger, R.E., Varyu, D.R., 2009. Geomorphic Analysis of the Skokomish River, Mason County, Washington. U.S. Bureau of Reclamation Report No. SRH-2009-22, Denver, CO (130 p).

Bountry, J.A., Oliver, K.J., Wille, K., 2011. 2-D hydraulic Modeling of Skokomish River Including Vance Creek. U.S. Bureau of Reclamation Report No. SRH-2011-10, Denver, CO (74 p).

Brandt, S.A., 2000. Classification of geomorphological effects downstream of dams. Catena 40, 375–401. https://doi.org/10.1016/S0341-8162(00)00093-X.

Brardinoni, F., Slaymaker, O., Hassan, M.A., 2003. Landslide inventory in a rugged forested watershed: a comparison between air-photo and field survey data. Geomorphology 54, 179–196. https://doi.org/10.1016/S0169-555X(02)00355-0.

Bretz, J.H., 1913. Glaciation of the Puget Sound region. Washington Geological Survey Bulletin No. 8 (244 p).

Castro, J.M., Jackson, P.L., 2001. Bankfull discharge recurrence intervals and regional hydraulic geometry relationships: patterns in the Pacific Northwest, USA. J. Am. Water Resour. Assoc. 37, 1249–1262. https://doi.org/10.1111/j.1752-1688.2001.tb03636.x.

Church, M., Ryder, J.M., 1972. Paraglacial sedimentation: a consideration of fluvial processes conditioned by glaciation. Geol. Soc. Am. Bull. 83, 3059–3072. https://doi.org/10.1130/0016-7606(1972)83[3059:PSACOF]2.0.CO;2.

Church, M., Slaymaker, O., 1989. Disequilibrium of Holocene sediment yield in glaciated British Columbia. Nature 337, 452–454. https://doi.org/10.1038/337452a0.

Collins, B.D., Dunne, T., 1989. Gravel transport, gravel harvesting, and channel-bed degradation in rivers draining the southern Olympic Mountains, Washington, USA. Environ. Geol. 13, 213–224. https://doi.org/10.1007/BF01665371.

Collins, B.D., Montgomery, D.R., 2011. The legacy of Pleistocene glaciation and the organization of lowland alluvial process domains in the Puget Sound region. Geomorphology 126, 174–185. https://doi.org/10.1016/j.geomorph.2010.11.002.

Cummans, J.E., 1973. Flood profiles and inundated areas along the Skokomish River, Washington. U. S. Geological Survey Water-Resources Investigations Report 62–73 https://doi.org/10.3133/wri7362 (20 p).

Cuo, L., Lettenmaier, D.P., Alberti, M., Richey, J.E., 2009. Effects of a century of land cover and climate change on the hydrology of the Puget Sound basin. Hydrol. Process. 23, 907–933. https://doi.org/10.1002/hyp.7228.

Curran, J.C., 2016. Geomorphic analysis of the Skokomish River system. Report to City of Tacoma Public Utilities, Tacoma, Washington, October 2016.

Curtis, K.E., Renshaw, C.E., Magilligan, F.J., Dade, W.B., 2010. Temporal and spatial scales of geomorphic adjustments to reduced competency following flow regulation in bedload dominated systems. Geomorphology 118, 105–117. https://doi.org/10.1016/j.geomorph.2009.12.012.

Czuba, J.A., Czuba, C.R., Magirl, C.S., Voss, F.D., 2010. Channel-conveyance capacity, channel change, and sediment transport in the lower Puyallup, White, and Carbon Rivers, western Washington. U.S. Geological Survey Scientific Investigations Report 2010–5240 https://doi.org/10.3133/sir20105240 (104 p).

Czuba, J.A., Magirl, C.S., Czuba, C.R., Grossman, E.E., Curran, C.A., Gendaszek, A.S., Dinicola, R.S., 2011. Sediment load from major rivers into Puget Sound and its adjacent waters. U.S. Geological Survey Fact Sheet 2011–3083 https://doi.org/10.3133/fs20113083 (4 p).

Dragovich, J.D., Logan, R.L., Schasse, H.W., Walsh, T.J., Lingley Jr., W.S., Norman, D.K., Gerstel, W.J., Lapen, T.J., Schuster, J.E., Meyers, K.D., 2002. Geologic map of Washington, northwest quadrant. Washington Division of Geology and Earth Resources Geologic Map GM-50.

Duan, N., 1983. Smearing estimate: a non-parametric retransformation method. J. Am. Stat. Assoc. 78, 605–610.

Dunn, B.C., 1941. Survey of the Skokomish River, Wash. U.S. House [of Representatives] Documents, Examinations of rivers and harbors, 78th Congress, 1st Session (1943). U.S. Government Printing Office, pp. 4–22.

East, A.E., Pess, G.R., Bountry, J.A., Magirl, C.S., Ritchie, A.C., Logan, J.B., Randle, T.J., Mastin, M.C., Minnear, J.T., Duda, J.J., Liermann, M.C., McHenry, M.L., Beechie, T.J., Shafroth, P.B., 2015. Large-scale dam removal on the Elwha River, Washington, USA: river channel and floodplain geomorphic change. Geomorphology 246, 687–708. https://doi.org/10.1016/j.geomorph.2014.08.028.

Easterbrook, D.J., 1964. Void ratios and bulk densities as means of identifying Pleistocene tills. Geol. Soc. Am. Bull. 75, 745–750. https://doi.org/10.1130/0016-7606(1964)75[745:VRABDA]2.0.CO;2.

Eronen, M., Kankainen, T., Tsukada, M., 1987. Late Holocene sea-level record in a core from the Puget Lowland, Washington. Quat. Res. 27, 147–159. https://doi.org/10.1016/0033-5894(87)90073-1.

Gendaszek, A.S., Magirl, C.S., Czuba, C.R., 2012. Geomorphic response to flow regulation and channel and floodplain alteration in the gravel-bedded Cedar River, Washington, USA. Geomorphology 179, 258–268. https://doi.org/10.1016/j.geomorph.2012.08.017.

Gilbert, G.K., 1917. Hydraulic-mining debris in the Sierra Nevada. U.S. Geological Survey Professional Paper 105 https://doi.org/10.3133/pp105 (154 p).

Grant, G.E., 2012. The geomorphic response of gravel-bed rivers to dams: perspectives and prospects. In: Church, M., Biron, P.M., Roy, A.G. (Eds.), Gravel-Bed Rivers: Processes, Tools, Environments. John Wiley & Sons, Ltd, Chichester, UK https://doi.org/10.1002/9781119952497.ch15.

Grant, G.E., Schmidt, J.C., Lewis, S.L., 2003. A geological framework for interpreting downstream effects of dams on rivers. In: O'Connor, J.E., Grant, G.E. (Eds.), A Peculiar River. American Geophysical Union, Washington, DC https://doi.org/10.1029/007WS13.

Griffiths, G.A., 1993. Sediment translation waves in braided gravel-bed rivers. J. Hydraul. Eng. 119, 924–937. https://doi.org/10.1061/(ASCE)0733-9429(1993)119:8(924).

Grossman, E.E., Curran, C.A., Rubin, S., 2015. Habitats and Sediment Transport to Inform Estuary and Salmon Recovery, Skokomish River-Delta, Washington: Final Project Report for Task 5 NWIFC 11EPA PSP430 "Monitoring of the Skokomish Estuary" (123 p).

Jacobs and Ober, 1925. Consulting Engineers. Skokomish River Improvement, Preliminary Report by Jacobs and Ober, Consulting Engineers, Seattle, WA, to Board of County Commissioners. Mason County, Washington (73 p).

Jacobson, R.B., Gran, K.B., 1999. Gravel sediment routing from widespread, low-intensity landscape disturbance, Current River Basin, Missouri. Earth Surf. Process. Landf. 24, 897–917. https://doi.org/10.1002/(SICI)1096-9837(199909)24:10<897::AID-ESP18>3.0.CO;2-6.

James, L.A., 1991. Incision and morphologic evolution of an alluvial channel recovering from hydraulic mining sediment. Geol. Soc. Am. Bull. 103, 723–736. https://doi.org/10.1130/0016-7606(1991)103<0723:IAMEOA>2.3.CO;2.

James, L.A., 1997. Channel incision on the lower American River, California, from streamflow gage records. Water Resour. Res. 33, 485–490. https://doi.org/10.1029/96WR03685.

James, L.A., 2006. Bed waves at the basin scale: implications for river management and restoration. Earth Surf. Process. Landf. 31, 1692–1706. https://doi.org/10.1002/esp.1432.

Jay, D.A., Simenstad, C.A., 1996. Downstream effects of water withdrawal in a small, high-gradient basin: erosion and deposition on the Skokomish River delta. Estuaries 19, 501–517. https://doi.org/10.2307/1352513.

Jones, E.E., 1925. Reconnaissance Survey of North and South Forks Skokomish River, Washington [map] U.S. Geological Survey, Washington, DC.

Juracek, K.E., 2000. Channel stability downstream from a dam assessed using aerial photographs and stream-gage information. J. Am. Water Resour. Assoc. 36, 633–645. https://doi.org/10.1111/j.1752-1688.2000.tb04293.x.

KCM, Inc, 1997. Skokomish River Comprehensive Flood Hazard Management Plan, Volume 1. Prepared for Mason County Department of Community Development, February 1997.

Knighton, A.D., 1989. River adjustment to changes in sediment load: the effects of tin mining on the Ringarooma River, Tasmania, 1875-1984. Earth Surf. Process. Landf. 14, 333–359. https://doi.org/10.1002/esp.3290140408.

Knighton, D., 1998. Fluvial Forms and Processes: A New Perspective. Hodder Arnold, London, UK (383 p).

Knowles, S.M., Sumioka, S.S., 2001. The National Flood-Frequency Program—methods for estimating flood magnitude and frequency in Washington, 2001. U.S. Geological Survey Fact Sheet 016-01 https://doi.org/10.3133/fs01601 (4 p).

Lee, S.-Y., Mauger, G., Binder, L.W., 2015. Climate change impacts on Tacoma Power watersheds. Report Prepared for Tacoma Power by the Climate Impacts Group, University of Washington, Seattle, June 2015 (44 p).

Legg, N.T., Heimburg, C., Collins, B.D., Olson, P.L., 2014. The channel migration toolbox: ArcGIS tools for measuring stream channel migration. Washington Department of Ecology Publication 14-06-032. https://fortress.wa.gov/ecy/publications/SummaryPages/1406032.html, Accessed date: 24 October 2016.

Leonard, C., Legleiter, C., Overstreet, B., 2017. Effects of lateral confinement in natural and leveed reaches of a gravel-bed river: Snake River, Wyoming, USA. Earth Surf. Process. Landf. 42, 2119–2138. https://doi.org/10.1002/esp.4157.

Logan, R.L., 2003. Geologic map of the Shelton 1:100,000 Quadrangle, Washington. Washington Division of Geology and Earth Resources Open File Report 2003–15.

Madej, M.A., Ozaki, V., 1996. Channel response to sediment wave propagation and movement, Redwood Creek, California, USA. Earth Surf. Process. Landf. 21, 911–927. https://doi.org/10.1002/(SICI)1096-9837(199610)21:10<911::AID-ESP621>3.0.CO;2-1.

Madej, M.A., Ozaki, V., 2009. Persistence of effects of high sediment loading in a salmon-bearing river, northern California. Geol. Soc. Am. Spec. Pap. 451, 43–55. https://doi.org/10.1130/2009.2451(03).

Major, J.J., East, A.E., O'Connor, J.E., Grant, G.G., Wilcox, A.C., Magirl, C.S., Collins, M.J., Tullos, D.D., 2017. Geomorphic responses to dam removal in the United States—a two-decade perspective. In: Tsutsumi, D., Laronne, J.B. (Eds.), Gravel-Bed Rivers: Processes and Disasters. John Wiley & Sons Ltd., pp. 355–383 https://doi.org/10.1002/9781118971437.ch13.

National Oceanic and Atmospheric Administration (NOAA), 2018. National weather service hydrologic prediction service webpage for the Skokomish River near Potlatch. http://water.weather.gov/ahps2/crests.php?wfo=sew&gage=srpw1&crest_type=historic, Accessed date: 6 February 2018.

Nelson, A., Dube, K., 2015. Channel response to an extreme flood and sediment pulse in a mixed bedrock and gravel-bed river. Earth Surf. Process. Landf. 41, 178–195. https://doi.org/10.1002/esp.3843.

Perkins Geosciences, 2002. Cedar River gravel study phase 2 report. Report by Perkins Geosciences with Harper Houf Righellis, Inc., to U.S. Army Corps of Engineers, Seattle, Washington, and Jones & Stokes, Bellevue, Washington. August 2002 (55 p).

Perrin, N.K., Miller, H.L., Stamets, J., 2014. Historic American engineering record, Cushman No. 1, hydroelectric power plan. Report by Historical Research Associates, Inc. to the National Park Service, July 2014 (15 p).

Pfeiffer, A., Anderson, S.W., Collins, B.D., Montgomery, D., Istanbulluoglu, E., 2018. The unstable rivers and the stable ones: using historical records of channel geometry to understand the processes driving changes in flood hazards in the Pacific Northwest, USA. Abstract EP11E-2109 Presented at 2018 AGU Fall Meeting, Washington, DC., 10–14 Dec.

Pinter, N., Heine, R.A., 2005. Hydrodynamic and morphodynamic response to river engineering documented by fixed-discharge analysis, lower Missouri River, USA. J. Hydrol. 302, 70–91. https://doi.org/10.1016/j.jhydrol.2004.06.039.

Pinter, N., Thomas, R., Wlosinski, J.H., 2000. Regional impacts of levee construction and channelization, middle Mississippi River, USA. In: Marsalek, J., Watt, W.E., Zeman, E., Sieker, F. (Eds.), Flood Issues in Contemporary Water Management. Kluwer Academic, Boston, pp. 351–361.

Plummer, G.H., Plummer, F.G., Rankine, J.H., 1902. Map of Washington showing classification of lands, 1902. U.S. Geological Survey Professional Paper 5, Plate 1.

Rankine, J.W., Plummer, G.H., 1898. Map of western Washington showing classification of lands. U.S. Geological Survey, 19th Annual Report, Part V, Plate III.

Richert, E.B., 1984. Long, Long Ago in the Skokomish Valley of Mason County, Washington. Mason County Historical Society Publ. No. 4, Belfair, WA, p. 84.

Savage, W.Z., Morrissey, M.M., Baum, R.L., 2000. Geotechnical properties for landslide-prone Seattle-area glacial deposits. U.S. Geological Survey Open-File Report 00–228 https://doi.org/10.3133/ofr00228 (5 p).

Schmidt, J.C., Wilcock, P.R., 2008. Metrics for assessing the downstream impacts of dams. Water Resour. Res. 44, W04404. https://doi.org/10.1029/2006WR005092.

Schroeder, W.L., Alto, J.V., 1983. Soil properties for slope stability analysis; Oregon and Washington coastal mountains. For. Sci. 29, 823–833. https://doi.org/10.1093/forestscience/29.4.823.

Schumm, S.A., 1973. Geomorphic thresholds and complex response of drainage systems. In: Morisawa, M. (Ed.), Fluvial Geomorphology. Publications of Geomorphology. State University of New York, Binghamton, NY, pp. 299–310.

Simons & Associates, Inc, 1993. Geomorphic and sediment transport analysis of the Skokomish River. Report Prepared for City of Tacoma, Department of Public Utilities, Tacoma, Washington, August 1993 (76 p).

Simons & Associates, Inc, 1994. Draft Skokomish River sediment transport data report 1993–1994. Report prepared for City of Tacoma, Department of Public Utilities, Tacoma, Washington, August 1994 (277 p).

Simons, R.K., Simons, D.B., 1997. Is there a role for science in hydropower relicensing? In: Mahoney, D.J. (Ed.), Waterpower '97. Proceedings of the International Conference on Hydropower. Vol. 2. ASCE, pp. 915–924

Slater, L.J., Singer, M.B., 2013. Imprint of climate and climate change in alluvial riverbeds: continental United States, 1950-2011. Geology 41, 595–598. https://doi.org/10.1130/G34070.1.

Slater, L.J., Singer, M.B., Kirchner, J.W., 2015. Hydrologic versus geomorphic drivers of trends in flood hazards. Geophys. Res. Lett. 42, 370–376. https://doi.org/10.1002/2014GL062482.

Smith, S.G., Wegmann, K.W., 2018. Precipitation, landsliding, and erosion across the Olympic Mountains, Washington State, USA. Geomorphology 300, 141–150. https://doi.org/10.1016/j.geomorph.2017.10.008.

Sofield, D.J., Barnett, C., Reinhart, M.A., 2007. Channel migration and avulsion potential analyses, Skokomish River valley, Mason County, Washington. Report Prepared for Mason County, Shelton, Washington, February 2007.

Stover, S.C., Montgomery, D.R., 2001. Channel change and flooding, Skokomish River, Washington. J. Hydrol. 243, 272–286. https://doi.org/10.1016/S0022-1694(00)00421-2.

Tetra-Tech, 2007. Channel cross section surveys. Contract # W912DW-07-D-1001, Skokomish River/River Channel Survey.

Thomas, B.E., Hjalmarson, H.W., Waltemeyer, S.D., 1994. Methods for estimating magnitude and frequency of floods in southwestern United States. U.S. Geological Survey Open-File Report 93–419 https://doi.org/10.3133/wsp2433 (211 p).

U.S. Army Corps of Engineers (USACOE), 2014. Skokomish River basin, Mason County, Washington, Ecosystem Restoration, Draft Integrated Feasibility Report and Environmental Impact Statement. January 2014.

U.S. Department of Energy (USDOE), 2009. Settlement Agreement for the Cushman Project, FERC Project No. 460, January 12, 2009.

U.S. Department of Energy (USDOE), 2010. Final Environmental Impact Statement, Cushman Hydroelectric Project, Mason County, Washington (FERC Project No. 360), Washington. DOE/EIS-0456, October 2010 (360 p).

U.S. Forest Service, 2016. Age Class 2015 [GIS data], Olympic National Forest, PNW Region, USDA Forest Service. https://www.fs.fed.us/r6/data-library/gis/olympic/, Accessed date: 14 November 2016.

U.S. General Land Office, 1861. Field notes for Township 21 North, Range 4 East. https://www.blm.gov/or/landrecords/survey/ySrvy1.php, Accessed date: 3 November 2016.

U.S. General Land Office, 1878. Field notes for Township 23 North, Range 4 East. https://www.blm.gov/or/landrecords/survey/ySrvy1.php, Accessed date: 3 November 2016.

U.S. General Land Office, 1893. Field notes for Township 23 North, Range 5 East. https://www.blm.gov/or/landrecords/survey/ySrvy1.php, Accessed date: 3 November 2016.

Washington State Department of Conservation and Development, 1935. Map of lower Skokomish River valley, Situated Near Shelton, Washington, in Mason County. Scale 1 inch: 600 feet; August 8, 1935.

Washington State Department of Natural Resources (WADNR), 1997a. South Fork Skokomish Watershed Analysis, Appendix A: Mass Wasting.

Washington State Department of Natural Resources (WADNR), 1997b. South Fork Skokomish Watershed Analysis, Appendix E: Stream Channels.

Williams, G.P., Wolman, M.G., 1984. Downstream effects of dams on alluvial rivers. U.S. Geological Survey Professional Paper 1286 https://doi.org/10.3133/pp1286 (83 p).

Wood, R.L., 1976. Men, Mules, and Mountains. The Mountaineers Press, Seattle.